INSTITUTO SUPERIOR DE ENGENHARIA DE LISBOA

Departamento de Engenharia de Electrónica e Telecomunicações e de Computadores

Connected cars: communication between vehicles and infrastructure through visible light

Carlos Pestana

Dissertação para obtenção do Grau de Mestre
em Engenharia de Electrónica e Telecomunicações

Orientadores : Prof.ª Dr.ª Paula Louro
Prof.ª Dr.ª Manuela Vieira

Júri:

Presidente: Prof. Dr. António Serrador

Vogais: Prof. Dr. Manuel Barata
Prof.ª Dr.ª Manuela Vieira

December, 2022

INSTITUTO SUPERIOR DE ENGENHARIA DE LISBOA

Departamento de Engenharia de Electrónica e Telecomunicações e de Computadores

Connected cars: communication between vehicles and infrastructure through visible light

Carlos Pestana

Dissertação para obtenção do Grau de Mestre
em Engenharia de Electrónica e Telecomunicações

Orientadores : Prof.ª Dr.ª Paula Louro
Prof.ª Dr.ª Manuela Vieira

Júri:

Presidente: Prof. Dr. António Serrador

Vogais: Prof. Dr. Manuel Barata
Prof.ª Dr.ª Manuela Vieira

December, 2022

Aos meus familiares e amigos

Acknowledgments

I wish to express my gratitude to everyone who helped me during this dissertation.

First and foremost, I would like to thank my advisors Prof. Paula Louro and Prof. Manuela Vieira for all the guidance they gave me. My thanks goes to them for their all their knowledge, the critics, their professionalism and dedication.

I would also like to thanks the OptoEletronics laboratory for providing material and equipment for the measurements of the results obtained.

To my parents for all their support, incentive and patience. No words can express my eternal gratitude.

To my girlfriend for all the encouragement and support throughout this work. She was present all the way.

A special thanks to all my friends for all the encouragement, patience and kind words they all gave me. They were present during this journey by my side, giving me support and friendship.

Abstract

Due to increased traffic demand, Radio Frequency (RF) band is currently in low supply. Since Visible Light Communication (VLC) employs the visible light spectrum to transmit and encode data, it is a potential alternative wireless technology to consider. In recent years, this kind of technology has changed and advanced.

This thesis aims to characterize and test VLC-based communication links for use in traffic management systems. The primary infrastructure for regulating access to roads, traffic lights, will shortly be replaced by more effective ones to enhance traffic management.

Tetrachromatic white LEDs serve as the VLC link's transmitters and are used for both data transmission and lighting. The receiver is built on SiC:H/a-Si:H photodiodes, which have selective spectrum sensitivity.

Modulation On-Off Keying (OOK) is used to transmit the message in a seven-cell intersection scenario with a 64-bit frame structure and LEDs at each corner creating a nine-footprint cell.

Using a simulation tool, the footprints of each cell and the coverage map were obtained.

To demonstrate how the frame structure is constructed and sent, a trajectory was tested with the vehicle travelling from East to South.

Keywords:

Visible light communication, connected vehicles, LED, traffic control, optical sensor

Resumo

Devido ao aumento da procura de tráfego, a banda de radiofrequência (RF) está actualmente em baixa oferta. Uma vez que a Visible Light Communication (VLC) emprega o espectro de luz visível para transmitir e codificar dados, é uma potencial tecnologia sem fios alternativa a considerar. Nos últimos anos, este tipo de tecnologia tem mudado e avançado.

Esta tese visa caracterizar e testar ligações de comunicação baseadas em VLC para utilização em sistemas de gestão de tráfego. A infra-estrutura primária para regular o acesso às estradas, semáforos, será em breve substituída por outras mais eficazes para melhorar a gestão do tráfego.

Os LEDs brancos Tetrachromatic servem como transmissores da ligação VLC e são utilizados tanto para a transmissão de dados como para a iluminação. O receptor é construído em fotodíodos SiC:H/a-Si:H, que têm sensibilidade de espectro selectivo.

A modulação On-Off Keying (OOK) é utilizada para transmitir a mensagem num cenário de intersecção de sete células com uma estrutura de 64 bits e LEDs em cada canto criando uma célula de nove pés de impressão.

Utilizando uma ferramenta de simulação, foram obtidas as pegadas de cada célula e o mapa de cobertura.

Para demonstrar como a estrutura da moldura é construída e enviada, foi testada uma trajectória com o veículo a viajar de Este para Sul.

Palavras-chave:

Comunicação por luz visível, veículos conectados, LED, controlo de tráfego, sensor óptico

Contents

List of Figures

List of Tables

Acronyms

BER	Bit Error Rate
BSDF	Bidirectional scattering distribution function
CCT	Correlated Color Temperatures
CT	Computed tomography
ECU	Engine Control Unit
EMI	Electromagnetic Interference
FPS	Frames per Second
FSO	Free Space Optics
FWHM	Full Width at Half Maximum
ID	Differentiable identification
IM	Intersection Manager
IR	Infrared
ISI	Inter Symbol Interference
LED	Light Emitting Diode
LoS	Line of Sight
L-VLC	Laser-Based Visible Light Communication
MRI	Magnetic resonance imaging
OFDM	Orthogonal Frequency Division Multiplexing
OMEGA	Home Gigabyte Access
OOK	On-Off Keying
OOK-NRZ	On-Off Keying Non-Return-To-Zero
OWC	Optical Wireless Communication
OWICELLS	Optical Wireless Networks for Flexible Car Manufacturing CELLS
RFI	Radio Frequency Interference

RGB	Red Green Blue
RONJA	Reasonable Optical Near Joint Access
SNR	Signal to Noise Ratio
SoC	System on a Chip
UAV	Unmanned Aerial Vehicle
UV	Ultra-Violet
V2I	Vehicle to Infrastructure
V2P	Vehicle to Pedestrian
V2V	Vehicle to Vehicle
V2X	Vehicle to Everything
VANET	Vehicular Ad Hoc-Network
VLC	Visible Light Communication

1

Introduction

As a major technological system today, transportation technologies, primarily vehicles, compute and sense a great deal of information. Vehicles of the last generation are equipped with various systems that allow them to perceive their surroundings, interact with other vehicles, and even interact with pedestrians. Therefore, the road infrastructures must also evolve in order to accommodate these communications, but this evolution is taking place at a slower pace [1].

The evolution of transportation systems and communication between vehicles and infrastructure is a well-invested area in terms of anticipated transformation. Using these types of communications will improve the safety and comfort of everyone on the road. This will also pave the way for new applications and technologies [1]. Figure 1.1 shows an example of these type of communications, that will be explained later in the Chapter 2.

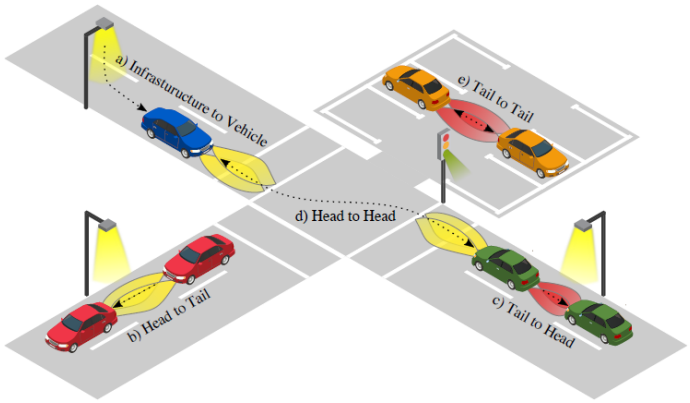

Figure 1.1: Vehicular VLC communication patterns in [1].

Optical Wireless Communication (OWC) is used to achieve this type of communication, and Visible Light Communication, or VLC, is the most commonly applied technology for vehicular communication. Recent studies and articles demonstrate how VLC has developed and paved the way for both indoor and outdoor environments. The field of light sources, mainly LEDs, has also seen a significant transformation over the last decade. This is because it is the primary transmission source of light, that can also be used for illumination purposes [1].

The work proposed in this dissertation is part of the IDICA (IPL/2022/POSEIDON _ISEL) project.

1.1 Dissertion Goals

This dissertation's primary objective is the characterization and testing of VLC-based communication networks for use in road management applications.

To build and simulate a scenario where it is possible the share of information between vehicles and infrastructures through V2V, V2I and I2V communication.

1.2 Stucture of the report

The chapters of this work are organized as follows.

The study and investigation of this dissertation's primary technology are covered in Chapter 2. What a VLC system is, its drawbacks, benefits, several application areas, and the tools required to set up this kind of communication are all outlined.

The work on which this dissertation is based is described in Chapter 3, and some important themes related to the work are provided.

The use of the simulation software is covered in Chapter 4. It is explained and demonstrated how to use the suggested tool, as well as the scenario created using the planned work from Chapter 3 and the outcomes.

The experimental findings are covered in Chapter 5, where measurements such a coverage map, footprint map, and tested scenario are described.

The key conclusions and a recommendation for future work are offered in Chapter 6.

2

State of the Art

Different ways of communicating and transmitting data have been emerging and evolving these past years. Many of these technologies are part of Optical Wireless Communication (OWC), and one of them is Visible Light Communication (VLC).

In this chapter, the history and evolution of VLC and some recent developments of this technology are presented, as well as some challenges that this application has. Finally some optical receptors and light sources will be discussed.

2.1 Evolution and applications of VLC

VLC, which is a technology of OWC, has a long engineering history, like RF engineering. In the past, before the innovation of VLC and other communication technologies, light was used differently to communicate, namely, through smoke signals, beacon fires, lighthouses, and signal markers. These were ways of visual communication used by human beings to communicate across long distances using light [2].

It was only in 1880 that the first experimental setup of VLC was achieved. Designed by Alexander Graham Bell, this project was known as Photophone. This prototype used a sunbeam reflected on a small mirror to transfer voice. In detail, the incoming sunlight is focused through a lens on a mirror, which is vibrating due to a person speaking through a mouthpiece. The light beams reflected from

the vibrating mirror contain the modulated speech signal. This information could be transmitted over a distance of 200 m. The Photophone is shown in Figure 2.1 [3].

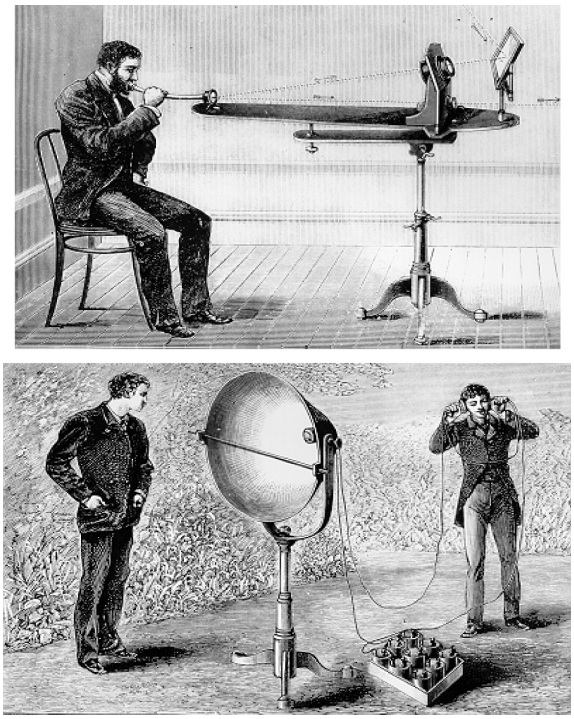

Figure 2.1: Alexander Bell's Photophone developed in 1880 [3].

After this innovation, new ways of transmitting information using natural light or artificial light continued. Until 1979, when F.R Gfeller and G.Bapst found a way to communicate indoor using Infrared (IR) Light Emitting Diodes (LED). Although this new development was far from perfect, it showed the potential of indoor OWC. During the following years, the LED industry advanced due to the development of fast devicesswitching, enabling fast modulations, in comparison to the fluorescent lamps and other light sources. This enabled several researches on high-speed VLC [4].

It was not until 1999, that it was proposed to used LED traffic lights as an optical signal transmitter, that later on it was investigated the possibility of using white LEDs for VLC system at relatively low rates [5].

Finally in 2009, VLC emerged as an alternative to aid the radio spectrum. This was due to the fact that the mobile industry was exponentially increasing, so the demand was high to obtain good quality services and high-speed data services [6]. The LED at this point was being explored for its good capabilities and higher spectral efficiency. So with a analogue equalizer, it was possible to obtain a data

rate of 100 Mbps with a on-off keying non-return-to-zero (OOK-NRZ) modulation [6].

During the following years VLC technology was refined and improved, to more recent developments like Reasonable Optical Near Joint Access (RONJA) in [7].

This technology [7] is an application of Free Space Optical (FSO) wireless communication, this system was developed and it is one of the best applications of FSO in the market. This project is a full-duplex point-to-point communication, this system uses LASER beams as the light source transmission, capable of establishing connection at a range of 1.4 km, reaching bitrates of 10 Mbps.

This technology [7] has many applications, like home and building security, individual and corporate internet connection and public networks. For this the functioning of RONJA, it is needed an optical transmitter installation and also a receiver frame installation, these are mounted on rooftops using coaxial cables with a protocol translator.

Another recent development is Home Gigabyte Access (OMEGA). OMEGA is a project developed for a home access network, capable of services up to 1 Gbps for wire links, power line communications, and wireless communications with ceiling LEDs, these three principal technologies of OMEGA can all provide high bandwidth. The OMEGA project has the goal to provide ultra-broadband home area networks. OMEGA has a new standard that consists of a wireless connection from the end-user [8]. The OMEGA concept can be shown in Figure 2.2.

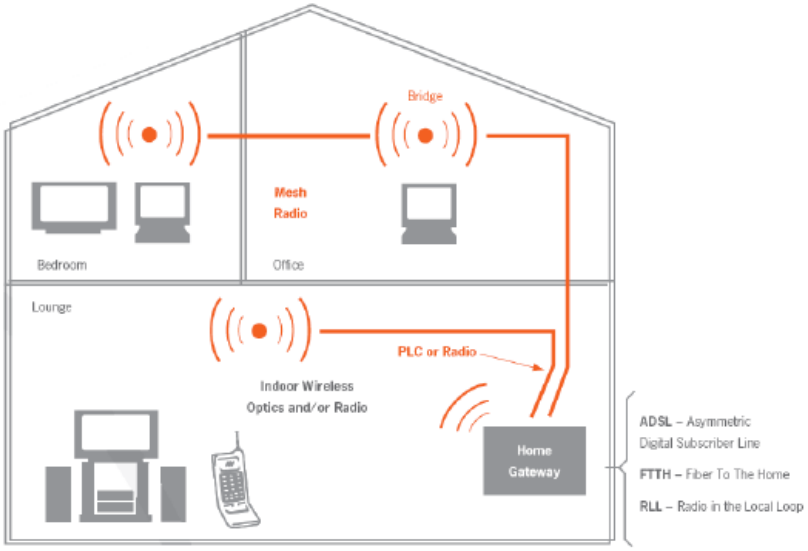

Figure 2.2: OMEGA home network concept [8].

At the moment, VLC has many applications areas, these systems can be applied

in various situations, for example, for home, industrial, vehicle, hospital and military applications. For all these applications the main OWC used is VLC.

2.1.1 Home

For home applications, visible light communication technologies are a good inexpensive option. Unlike RF technologies, it does not require an expensive RF band and it is easy to implement, making VLC a good option for home applications. At home, any light source can be used to transmit information, and with sensors, light can be used to monitor and control data and illumination lighting. This light can be used for every gadget at home, like computers, smartphones, printers, tablets, for many new home appliances technologies and applications. The Figure 2.3 shows a smart lighting office project of Boston University with communications with a high data rate using VLC technology [2].

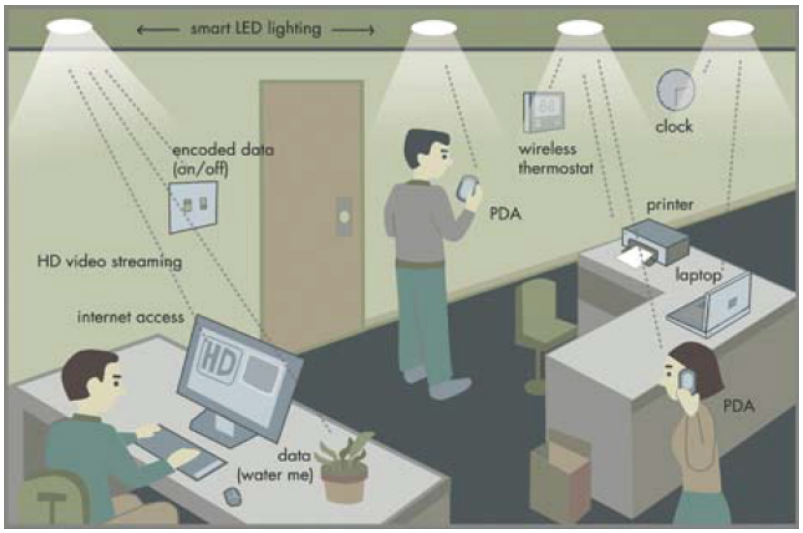

Figure 2.3: Boston Smart lighting office [2].

2.1.2 Hospitals

For hospital, or medical usage, these technologies must work, and they must be protected from miscalculations since these devices are for people's health. One factor that can these medical devices need isolation from is interference, mainly Electromagnetic Interference (EMI), also called Radio Frequency Interference (RFI). Since VLC does not produce interference like EMI or RFI, it is a good option for hospital use. The mentioned interference is harmful to hospital

equipment such as Computed tomography (CT) scans, also known as CT scans or Magnetic resonance imaging (MRI) scanners, also known as MRI scanners [9].

Another device that was developed is an autonomous robot named HOSPI, that uses VLC technology to carry medical supplies and equipment. This robot is shown in Figure 2.4 [10].

Figure 2.4: Mobile robot HOSPI [10].

2.1.3 Industrial

VLC has many recent applications and technologies in the industrial business. In 2018 a project named Optical WIreless networks for flexible car manufacturing CELLS (OWICELLS) investigated the use of VLC systems for the manufacturing of automotive cells. This system has low latency and uses IR LEDs after switching from phosphor-coated blue LED chips. Although Red, Green, and Blue (RGB) LEDs can be used to achieve high data rates. VLC is used in industrial areas for indoor communication and localization in areas where there are inflammable products [11].

2.1.4 Military

For military purposes, there is a project developed to transmit encrypted data between military bases using a VLC system with the help with a tactical drone, also named Unmanned Aerial Vehicle (UAV). This drone has a laser equipped

and it flies to the desired near military station to deliver the encrypted message to the end node, while in the air. This system requires a receiver circuit designed for this purpose, typically using a solar panel, and since the drone has a laser this is a Laser-based Visible Light Communication (L-VLC) system [12]. The Figure 2.5 illustrates the L-VLC system.

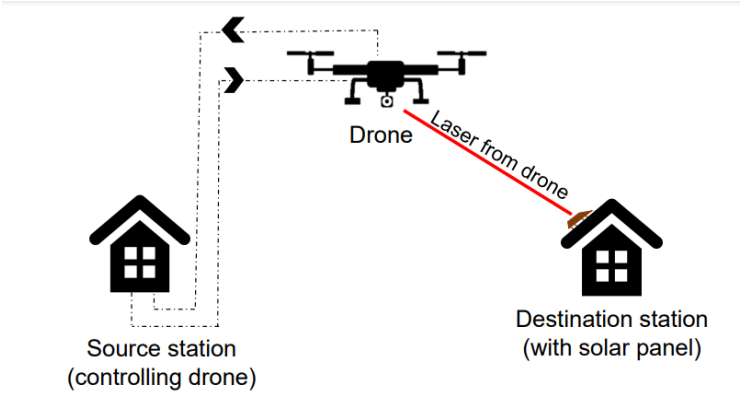

Figure 2.5: Point-to-point L-VLC data transmitting system using a UAV [12].

2.2 VLC in Autonomous Technology

In this Section, it is going to be discussed the main technology of this dissertation, which is VLC in autonomous technology.

This technology has been increasing in the last few years, with improvements in safety and comfort in driving. A type of communication between vehicles, infrastructure and even pedestrians, called Vehicle-to-Vehicle (V2V), Vehicle-to-Infrastructure (V2I) and Vehicle-to-Pedestrian (V2P) can reduce accidents. It is also referred to as Vehicle-to-Everything (V2X).. Accidents can be prevented with this type of communication, by exchanging information and warn vehicles and pedestrians about potential dangerous situations. This communication is illustrated in Figure 2.6.

Nowadays traffic lights and vehicles already use LEDs, making it easier to implement systems with VLC. So vehicles with LEDs can communicate with each other, at high speed and with low latency, in comparison with RF-based systems. One possible V2V communication is by using a Vehicular Ad hoc-Network (VANET). This system can create a wireless path to allow the exchange of data between vehicles [13]. However, there are some issues with this technology, one of them

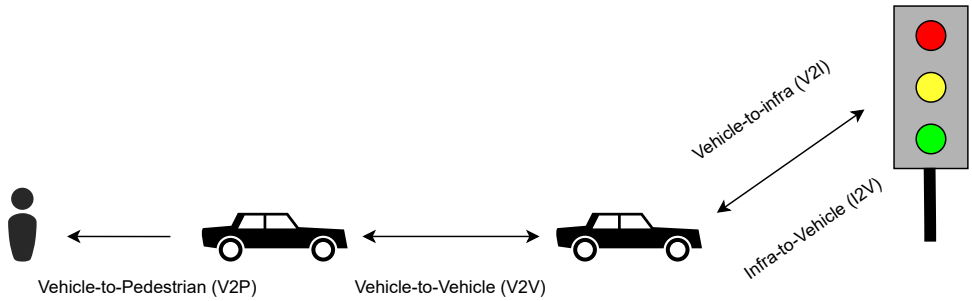

Figure 2.6: VLC in Autonomous Communication.

being the need to keep line of sight (LoS) between the VLC receiver and transmitter, so that the modulated light can reach the desired receiver, usually being a photodiode connected to a transimpedance circuit, to convert the current from the receiver to voltage. Another problem is the noise, in comparison to indoor VLC communication, the outdoors has more factors to degrade the source signal, since the communication channel distance is more extensive. Furthermore, the receiver and emitter are in constant movement since they are implanted in cars, so the distance and light emitting angles are always changing. Another unpredictable aspect of this is the weather, this factor can influence the emitted light, since it can reflect it or block it completely [14].

In [13] a car-to-car communication system was implemented using VLC, which uses the car as a transmitter and a receiver. The information sent is from reading the Engine Control Unit (ECU), and it contains the vehicle speed, gas, and brake step depth, which then is sent to another car by VLC and infrared. This system is shown in Figure 2.7.

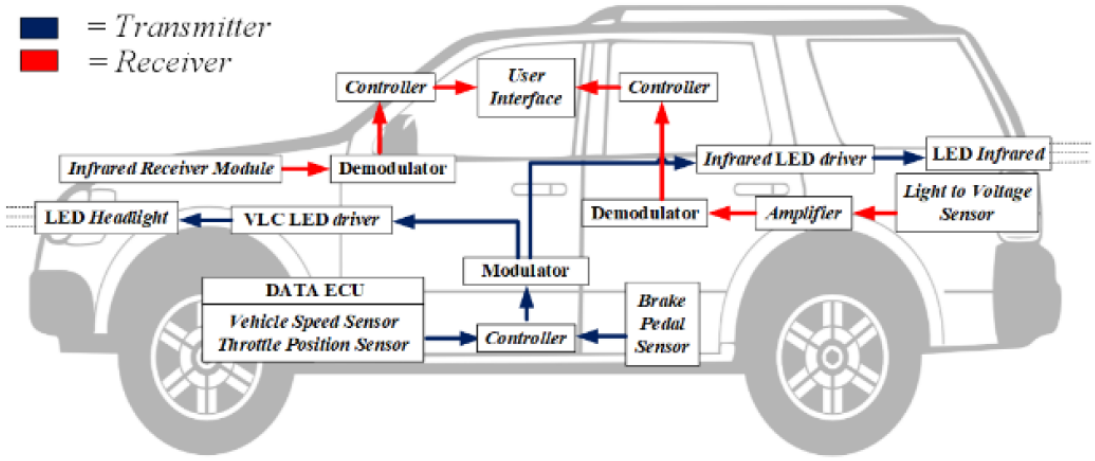

Figure 2.7: Overall System Design for car-to-car communication in [13].

After several test scenarios done in [13], is it important to use an adequate sensor for the VLC system, since some can not be used during the day, because of the interference created by the sun waves. Also, the communication distance is larger at night and the optimal reception angles are 0° and 25°. Lastly, rainwater does not affect the VLC communication, so it is still possible to trade information during rainy days however, lights from other vehicles and other sources are harmful to the light signal creating noise.

In [15] a V2X communication was simulated, in form of a traffic light-controlled crossroad. The goal of this simulation is to show the efficiency and safety increase that happens when this system is implemented in a intersection. The information is sent to various vehicles about the status of the traffic and overall information of the road by sending coded signal by a VLC system, that then is later decoded in the vehicle receiver circuit. The Figure 2.8 shows the simulated traffic intersection.

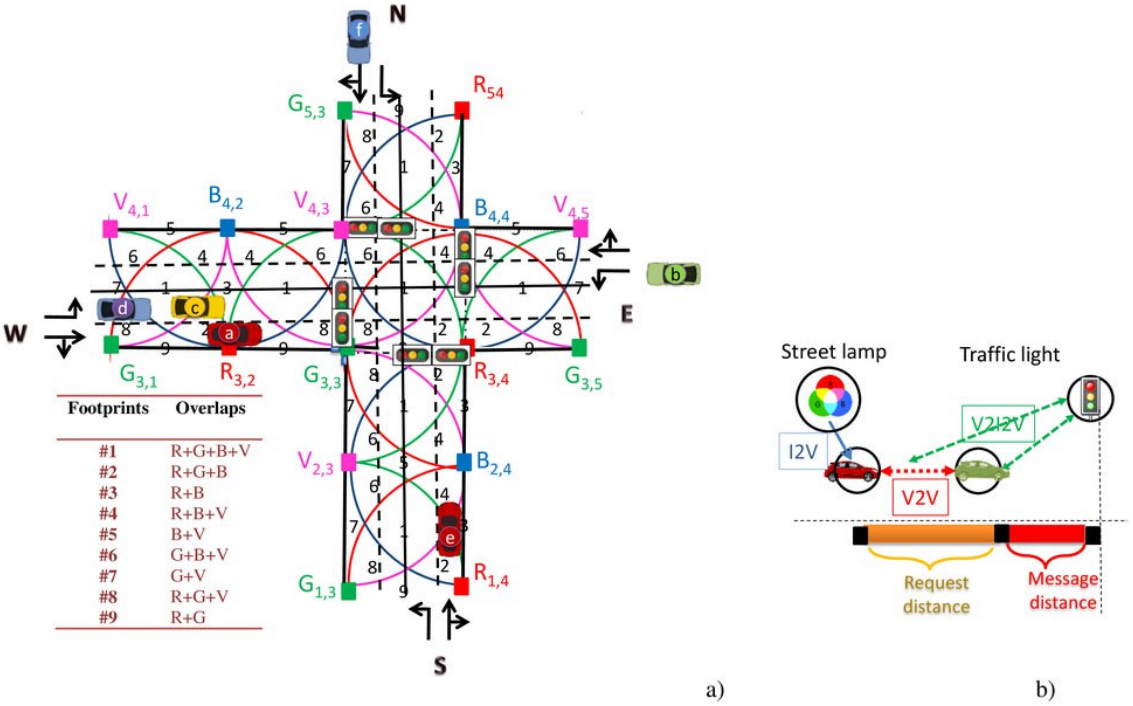

Figure 2.8: Simulation executed: (a) V2X lighting plan model, (b) Graphical representation of the simultaneous localization and mapping problem [15].

The LED array in this simulation has several nodes that send information in synchronism and with traffic information so that when a vehicle approaches the node, the message is sent. However, each node has its RBGV color with its array position, which is installed at the roadside. It is proposed in this VLC system

that the receiver circuit has a photodiode based on a tandem heterostructure between two contacts. Also, the optical sources used are commercial RBG white LEDs and each node possesses, as mentioned, an RBGV LED, however only one is modulated for transmitting information, while the others only are necessary for white light [15].

2.3 Challenges of VLC

VLC systems have many advantages, some of which were already mentioned in the past sections. However, VLC still have many challenging factors that harm the overall system. In this Section, several problems are going to be listed and discussed.

2.3.1 Line of Sight (LoS)

LoS is one factor that is important in VLC systems, meaning that the source light from the transmitter is emitting directly into the receiver, since the signal is stronger this way, being one of the advantages of VLC. However, light can pass through some objects but not all, some of them can only reflect light, which is a coverage disadvantage. These reflected lights can still reach the receiver, but the signal will be much weaker since some of the energy is absorbed by the object when reflected. Even though the reflected light is weaker, it can still hold enough power for communication, if the photoreceiver is sensitive enough. So to get a strong VLC signal the LoS must be maintained, and the light cannot be reflected or blocked [16].

2.3.2 Multipath Fading

As said in the LoS Subsection, certain objects can reflect light, which means reflecting the message trasmitted by the light source, and since LEDs have a wide beam when transmitting information, meaning a higher Full Width at Half Maximum (FWHM), this creates a problem where the same signal reaches the receiver at different time delays, which is Multipath Fading. One way to try to solve this problem is to implement Inter Symbol Interference (ISI), however, this implementation will decrease the performance of the VLC system. [17].

2.3.3 Ambient Light Interference

Ambient light can be a source of noise and interference, especially when the transmitter uses wide beam transmission, which makes the ambient light more damaging to the VLC system. And since the ambient light interference changes depending on the time of day, this leads to variations of the Signal to Noise Ratio (SNR), which is a problem for VLC. Due to this, it is necessary to have better quality receivers to separate these low SNR signals, which attenuates the signal and increases the cost of the system [17].

2.3.4 Simplex Communication

A VLC system can be implemented in a downlink or uplink direction, although uplink connections are more challenging to implement, so VLC systems are better used for downlink connections due to lower cost and better bandwidth [18]. In these circumstances the communication is simplex, meaning, the communication channel is unidirectional, so there are no guarantees that the message was successfully received, since the receiver cannot send a confirmation message.

2.3.5 Lights ON

For VLC systems it is required to have a light source for the transmitter and it needs to be on for communication. For industrial and commercial purposes, there is always a need for illumination, so it is not a problem for these applications since the sources are on. However, for home applications during the day, the light sources are off since there is no need for illumination, after all the lights sources need to be dimmed up and down to be able to send information. So due to this problem, there must be solutions, and in [19] it is studied ways to communicate in "lights off" mode. To be able to communicate in this mode, it is necessary to tune down the light source to a level perceptibly "off" to human eyes and to do this, it is necessary to keep into account various factors, for example, the ambient brightness, because the ambient light changes based on the time of the day. This factor influences the illumination of surfaces within the room, and also the clarity of the sources under direct viewing, which are both important criteria in communicating in "lights off" mode [19].

2.4 VLC Receivers

It is necessary to have a light source coupled to a transmitter circuit that transmits the signal to a sensor or a photodetector for processing. A typical VLC system can use two types of VLC receivers, as explained in this subsection.

2.4.1 Photodetector

A photodetector, also known as a photodiode or non-imaging receiver, is a component, namely, a semiconductor, that captures light and converts it into an electric signal, by converting each captured photon into a free electron, ideally. In these devices, light can be sampled at rates as high as tens of megahertz [20]. Photodiodes are based on PN junctions. In spite of this, it is reversely biased. In the absence of a signal, there is only a small reverse current flowing through the diode. During the photodetection process, photodetectors generate noise, which increases the SNR of the VLC system, thus reducing its performance. Shot noise, thermal noise, and dark-current noise are the main sources of noise. Despite the fact that thermal and dark-current noise can be reduced, shot noise cannot be reduced because it is intrinsic to the photodetection process [21].

2.4.2 Imaging Sensor

There is another type of receiver, named imaging sensor or camera sensor. This type of sensor is present in most recent smartphones that can capture videos and images. This factor increases the potential of VLC systems since this type of sensor is common and can turn any device into a VLC receiver. An imaging sensor has many photodetectors, present in an integrated circuit or a matrix, and unlike the traditional photodetectors, it is limited by its low frames per second (FPS) if high-resolution photography is desired, although increasing the number of photodetectors, raises the fps.

In [22] it proposed the use of an image sensor receiver for a new automotive VLC system. It uses DCO-OFDM for more effective and flexible transmission. Throughout their work, several values of BER and data rate were achieved. However, the best result achieved is a data rate of 45 Mbps with a BER of 0, and also a higher data rate of 55 Mbps with a BER of $< 10^{-5}$. Figure 2.9 shows the proposed system.

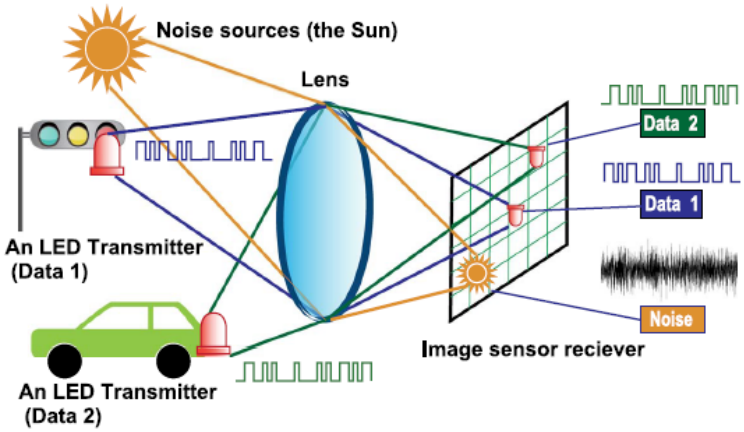

Figure 2.9: Image sensor receiving the information from multiple sources including noise from sun [22].

2.5 Transmitter

A light source is needed for a VLC system to work since, it is this component that is sending the information, and the most common light source used is LEDs, although lasers can also be used in these systems, LEDs are superior in the market since they can also be used for illumination purposes.

A single LED may not sufficient to emit the same light as a fluorescent lamp, so it is necessary to use many LEDs operating at the same time, to enable the same output optical intensity. So for a VLC system, it is used a LED luminaire, which is composed of a LED bulb, housing, and some other components. The main component of this LED luminaire is the LED bulb, also known as an LED lamp. Inside of this bulb, there are multiple LEDs, and also a LED driver, that is responsible for controlling the LEDs driving currents that is given to the LEDs. This LED driver, is also responsible to modulate the light to be used in a VLC system. One type of modulation that is commonly used in these systems is On-Off Keying modulation. In this type of modulation, it is attributed two different levels of light intensity for the bits "0" and "1" when transmitted [20].

There are many types of LEDs, and each one has its purpose, for example, to be able to produce white light LEDs, it is necessary to use the RGB combination, which is mixing three separate LEDs, red, green, and blue. It is important to know what the human eye can perceive, so in the Figure 2.10 it is shown a range of frequencies, which shows the visible light range with the colors the human eye can perceive. The visible light spectrum range, goes from 430 THz to 790 Thz.

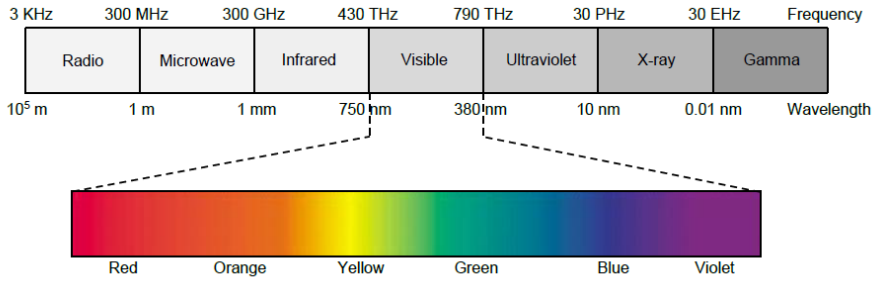

Figure 2.10: Range of frequency that the human eye can perceive, also known as the visible light spectrum [20].

2.5.1 Optical Sources

White LEDs are created by mixing light of various colours, primarily blue and yellow. A yellow phosphor is used to convert the blue phosphor emitted from the chip into yellow light, this mix of blue and yellow photons produces white light. However this created light comes with various correlated color temperatures (CCT) [23]. There are several techniques to enhance the white light spectrum, to provide a better quality of light. A typical white light spectrum can be seen in Figure 2.11 by showing a peak at around the wavelength of blue light and a high intensity of yellow light.

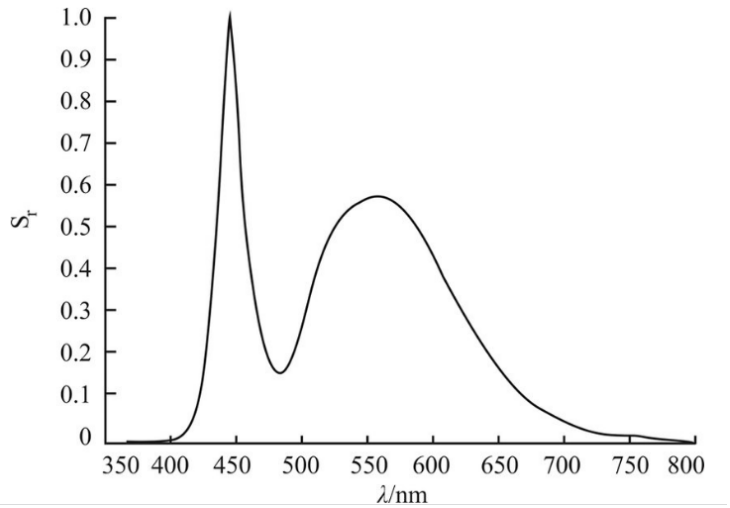

Figure 2.11: Typical phosphor white light spectrum [24].

There are other type of white LEDs, like RGB white LEDs. The white light spectrum is visible in Figure 2.12.

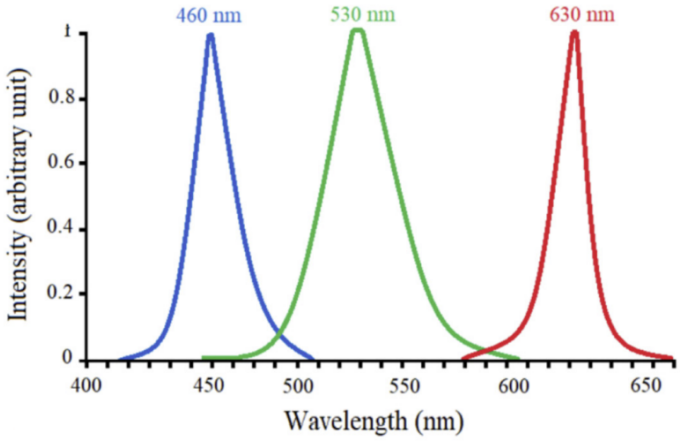

Figure 2.12: Typical RGB white light spectrum [25].

The spectrum of RBG white LED, there are three peaks, one for the red wavelength, one for the blue wavelength, and one for the green wavelength. In order to produce white light, these three diodes work simultaneously [25].

Each LED has its own characteristics and specifications, and white LEDs are no exception. For example, every LED has its FWHM value, wavelength forward voltage, etc. White LEDs require a minimum current at a certain voltage. For instance, [26] displays the current-voltage (I-V) of a white LED devoid of phosphor with a series resistance of 30 Ω, as displayed in Figure 2.13. This kind of graphic will vary according on the LED utilized.

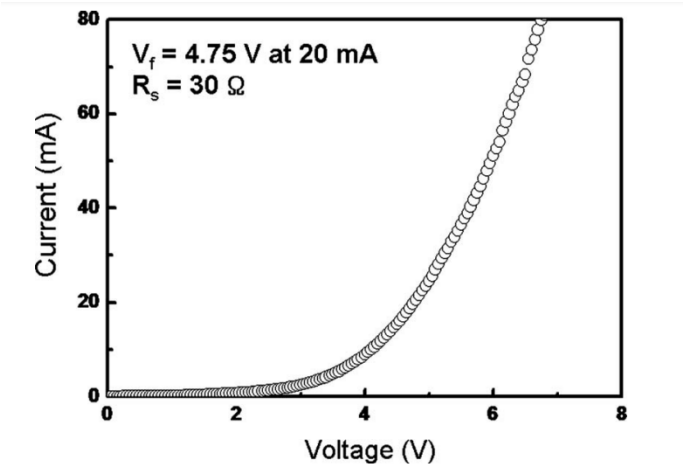

Figure 2.13: I-V characteristics of the white LED in [26].

2.5.2 Modulations

The VLC system quality depends on many factors, and one of them is the type of LED used. Since there are several LEDs for different purposes, the results are going to vary, especially when different modulations can be used. The type of modulation used in the VLC system can also affect the outcome. In the following Table 2.1 there are several proposed results, each one of them using its criteria.

Table 2.1: Review of proposed solutions of VLC based systems.

Ref	Type of LED	Type of Modulation	Data Rate [Mbps]	BER	Bandwidth [MHz]
[27]	White	16-QAM OFDM - analogic OOK - digital	1 and 8	-	4
[28]	White	OOK-NRZ	1000	7.36×10^{-4}	14 - 520
[29]	White	64-QAM DMT	2500	1×10^{-2} @ I = 150 mA, Vpp = 0.4 V	416
[30]	White	OFDM	2 - 12	8×10^{-3} @ SNR = 20 dB, R = 12 Mbps	-
[31]	Infrared	OOK	45×10^{-6}	0.0178 @ d = 3 m	-
[32]	UV	OFDM	1310/ 3320	2.46×10^{-3} / 2.1×10^{-3}	100

In [27] it is done experiments using a white LED with a blue filter and System on a Chip (SoC) based test-bed. The information was transmitted in both analog and digital modulation, using Orthogonal Frequency Division Multiplexing (OFDM) and On-off Keying (OOK) modulation, respectively. It is achieved a data rate of 1 Mbps for the analog modulation and 8 MBps for the digital one. It is also measured the Bit Error Rate (BER), in different data rate, through eyes diagrams, for the digital modulation.

In [28] it is proposed the use of a cascaded T-bridge pre-equalization circuit, to be used in an indoor environment in real time use at high speed links. The modulation used is OOK-NRZ. It is also used a blue filter, that was able to increase the -3

dB bandwidth from 14 MHz to 520 MHz, with a relatively low BER, at a distance of 1.5 m, with a data rate of 1 Gbps, in a real time VLC system.

In [29] it is also proposed a high speed white light, in real time, VLC system, based on a phosphorescent white LED. It was achieved a data rate of 2.5 Gbps, using 64-QAM DMT modulation, and achieved a bandwidth of 416 MHz. In this system, it is also used pre-equalization circuits are also investigated some factors that influence this circuit like, peak-to-peak voltage (V_{pp}) and the bias current of the white LED. It is shown that the BER varies with the bias current at different V_{pp} levels. The BER can be seen in Figure 2.14.

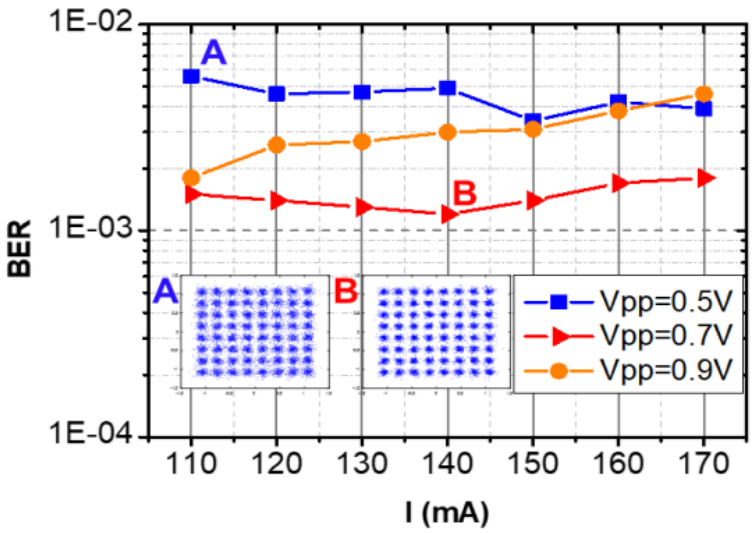

Figure 2.14: BER versus bias current of the white-light LED [29].

The use of a white LED with a blue and flattening filter is proposed in [30]. The communication link has a 1 m distance, and it was possible to achieve a maximum data rate of 12 Mbps. However, it was used several values for the data rate, to compare different values for the SNR and BER. These values can be seen in Figure 2.15.

It is proposed in [31], a low speed communication method, for an uplink channel using a VLC system, however, it is used an IR LED and the use of a camera as the receiver in an indoor environment. It is said that this proposed method can eliminate glare, flickering and other interference. The integrated camera is for surveillance and communication purposes, since it has dual use, it is highly energy efficient and low cost. Throughout this work, the frame rate was varied from 49 to 90 fps, at different resolutions. The BER is higher for longer communication distances, going up to 0.0178 at a distance of 3 m.

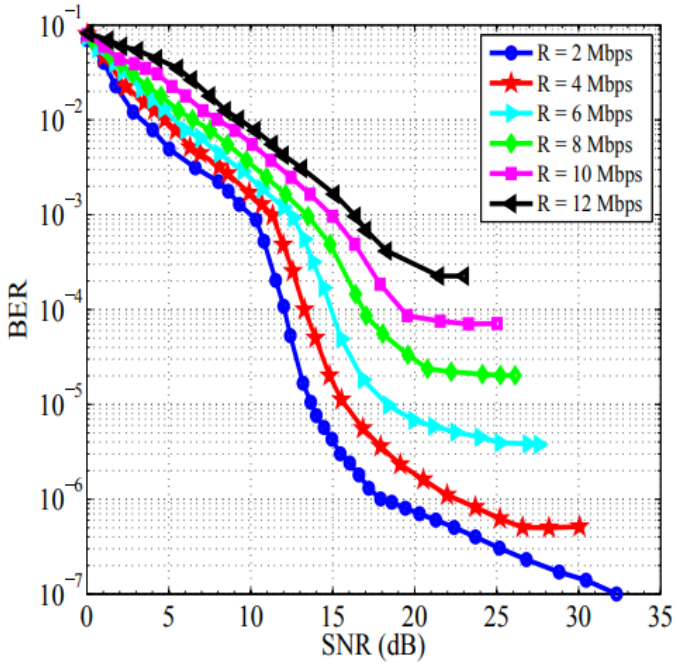

Figure 2.15: BER versus bias current of the white-light LED [30].

In [32] it is provided a baseline work for a VLC system that is capable of a maximum data rate of 3.32 Gbps, using OFDM modulation, with a Violet and Ultra-Violet (UV) μLEDs. The reason that μLEDs were used instead of conventional LEDs, is due to the fact that μLEDs are smaller, meaning that they can be driven to higher current values and bandwidths. In this work the bandwidth achieved was 100 MHz for the UV μLEDs and 130 MHz for the violet.

In table 2.2, it is summarized various modulation techniques as well as their advantages and disadvantages. Despite the fact that some modulation techniques provide high data rates and distances, they are costly and complex.

Table 2.2: Advantages and disadvantages of modulations [20] [33] [34] [35].

Modulation Techniques	Advantages	Disadvantages
OOK	• Simple, robust and easy to implement. • Requires lower power bandwidth. • Reduced power dissipation.	• Spectral efficiency limits. • Inter-symbol interference occurs at high data rates. • Operating at lower intensity levels, causes the LED to shift colors. • Low data rates, especially with different dimming levels.
OFDM	• Higher data rates. • Longer transmission distances. • It can deal with inter-symbol interference and multipath fading. • Multiple carrier transmission.	• Implementation poses many challenges.
CSK	• Overcomes limitations in data rates. • Ability to overcome dimming issues. • Specifically designed for VLC applications.	• Complex receiver module.
PPM	• High power efficiency. • Simple implementation.	• Compromised spectral efficiency. • Low data rates.
PWM	• The dimming process does not rely on pulse intensity levels. • Operating at lower intensity levels does not shift colors.	• Limited data rates. • In order to raise the data rates, a more complex system is necessary.

3

Proposed Work

It was stated in Chapter 2, that using VLC to connect vehicles and infrastructures will increase security and traffic flow in an intersection. The purpose of this chapter is to propose a traffic intersection scenario using VLC as a traffic control method. Navigation and road traffic control of the vehicle are required to make this possible. An example of this scenario is shown in Figure 3.1.

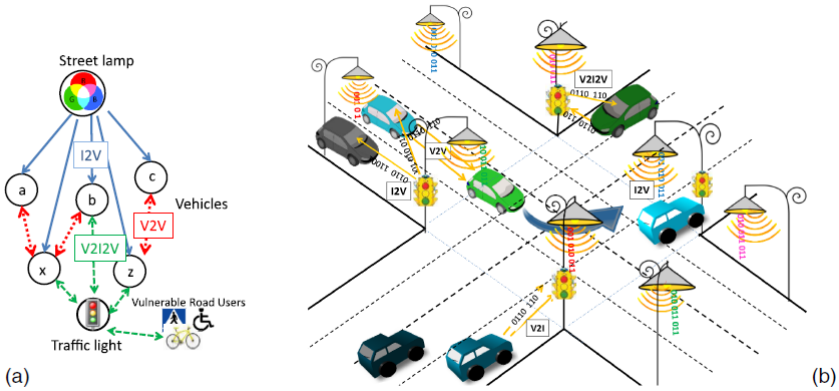

Figure 3.1: Illustration of the proposed I2V2V2I2V communication scenario: (a) generic model for cooperative vehicular communications. (b) Connected vehicles communication link [36].

According to the proposed scenario, there are several transmitters, such as streetlights and traffic signals, which are responsible for transmitting map information

and traffic messages to moving vehicles and each street light has its differentiable identifications (IDs). This data is encoded, modulated, and then converted into light. The receivers on the roof of the vehicle will capture this data. It is then possible to send information from one vehicle to another using its headlight (V2V), or to send a "request" to change routes to a crossroad receiver (V2I). Bi-direction communication (V2I2V) is established when the local controller emits the "response" message [15].

In communication and illumination, tetra chromatic white sources are used as transmitters, with different channels for each chip. In each LED node, only one chip transmits data, while the rest provides constant current for white perception. As a result, each transmitter $(X_{i,j})$ in the network is assigned a color X (R, G, B or V) and a horizontal and vertical ID position (i,j) [15].

This scenario was first discussed in chapter 2, where the Figure 3.2 was shown:

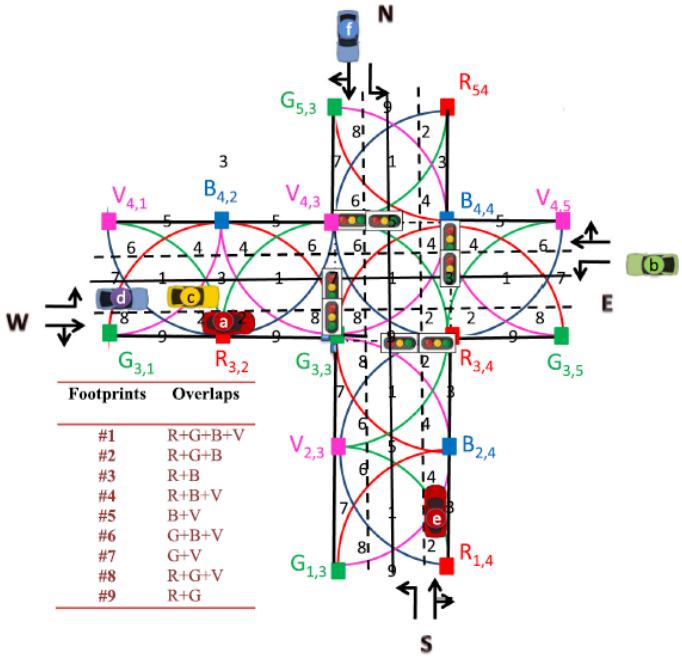

Footprints	Overlaps
#1	R+G+B+V
#2	R+G+B
#3	R+B
#4	R+B+V
#5	B+V
#6	G+B+V
#7	G+V
#8	R+G+V
#9	R+G

Figure 3.2: Simulation executed: V2X lighting plan model [15].

A joint footprint generated by a variety of vehicles in different traffic lanes and positions, each with their own destination, is shown in figure 3.2. Vehicles must be within the transmitter's transmission range to receive information. By overlapping the transmission range circle, there are nine possibilities. As well as locating and decoding the information, these footprints are important for locating the vehicle in the cell [15].

There is a message sent by each LED, which includes its synchronization, physical identification, and traffic information. As soon as a probe vehicle enters the node range, the receiver responds to the light signal and assigns it a unique ID and the traffic message. As each instant passes, the receiver identifies the footprint and stores the reference point [15].

It is necessary for a follower and a leader vehicle to exchange information in order to build a V2V system. It can then be sent to the next vehicle or infrastructure near it. Identifying the leader vehicle, which is the first vehicle on a lane, or the second if the first has started crossing an intersection, is crucial [36].

When approaching an intersection, drivers select the lane based on their destination, and at this point the vehicle sends a "request" message to the intersection manager (IM), which is an interconnected receiver. A confirmation message will be sent by the IM, if there is no risk of conflict with other vehicles. When the "confirmed vehicle" message is received, the driver must follow a specific footprint region [15] [36]. This process is shown in figure 3.3.

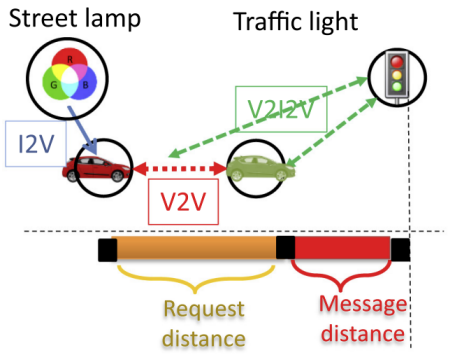

Figure 3.3: Graphical representation of the simultaneous localization and mapping problem [15].

3.1 Coding Techniques

Coding the information was done using OOK modulation. All messages in the frame start with the same synchronization header [10101], imposed simultaneously on all emitters in an ON-OFF pattern. Following this is the ID block, which specifies the location (x, y coordinates) of each emitter. In order to encode decimal numbers, ID cells use four-bit binary representations. If the message is sent by an IM transmitter, the identification code is followed by a pattern of [0000],

while if the message is a request, a pattern of [00] is used. The next block represents the steering angle δ, which represents the angle at which the vehicle is moving. Using this angle, the vehicle's goal can be determined. There is a corresponding number in the unit cell for each of these footprints. In most cases, the vehicle will not move along the same trajectory. The vehicle's heading will form an angle with the direction of travel as the vehicle moves toward its destination (e.g. turning right or left). An example of a two-dimensional coordinate system in a non-omnidirectional configuration is shown in Figure 3.4 a) , the Ackermann steering principle whose angle ϕ is defined by the target position ($\theta = \phi/2$) is illustrated on Figure 3.4 b), and Figure 3.4 c) shows the mentioned eight possible orientations [15].

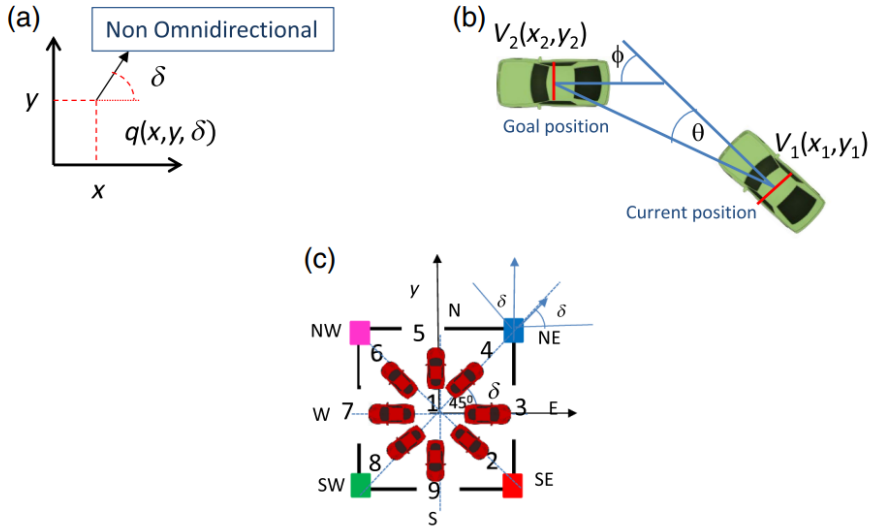

Figure 3.4: (a) Pose: q = (x,y, δ). (b) Ackermann steering principle. (c) Pose orientations (N, S, E, W, NE, SE, SW, and NW) [15].

The traffic message is the last message in the frame structure. An important point to remember is that every frame ends with a stop bit. Figure 3.5 shows an example of a frame structure when the car moves from north to south.

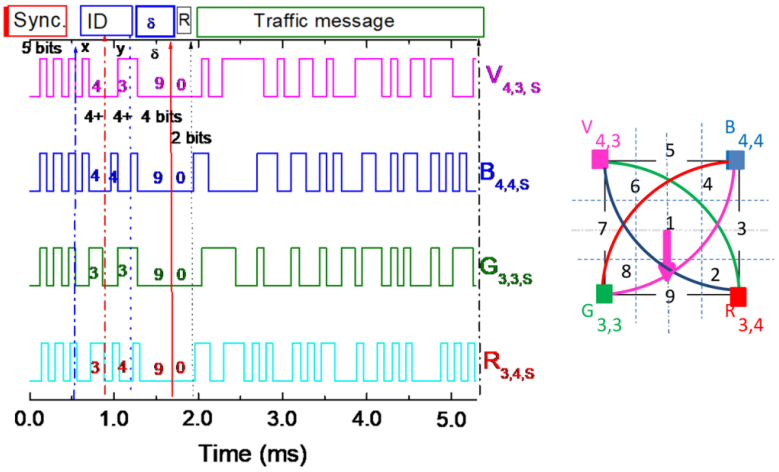

Figure 3.5: Frame structure representation of a request message [15].

3.2 Phasing diagram

It is common for more than one vehicle to cross an intersection at the same time. The phasing diagram in Figure 3.6 shows how the vehicle should maneuver to cross the intersection safely. The "green pose" is referred to as West straight, South left turn, and West turn. "Red poses" are south straight, east left, and south right. In turn, East straight, North left, and East right maneuvers correspond to "blue poses", while North straight, West left, and North right maneuvers correspond to "violet poses" [15]. This diagram can be seen in the Figure 3.6.

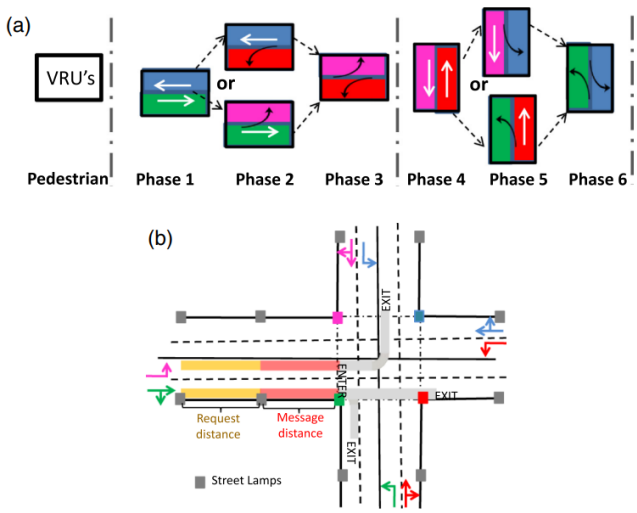

Figure 3.6: (a) Representation of phasing diagram. (b) Physical area and channelization [15].

Therefore, the vehicle must occupy the correct lanes, for example, if it intends to turn left, it must use the left lane. When turning right or driving straight, the vehicle must occupy the right lane. When approaching the intersection, there are two elements in the functional area: request distance and response distance. It is necessary to change lanes within the requested distance if lane changes are required [15].

3.3 Receiver

In [15], a double pin/pin a-SiC:H photodetector is used for the receiver. An a-SiC:H-n/a-SiH-n heterostructure with high resistance is used in this device. A schematic of this receiver can be found in Figure 3.7 [37].

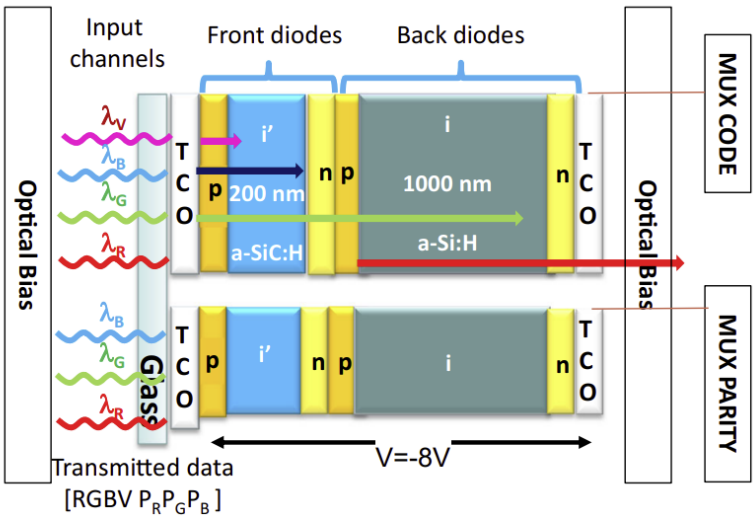

Figure 3.7: Receiver configuration in [15].

The receiver is like an active filter in that it absorbs long wavelengths in the back while confining short wavelengths in the front, while medium wavelengths are absorbed across both, as shown in Figure 3.7. Wavelengths higher than 550 nm are amplified, while wavelengths below 500 nm are quenched [37].

Its two main functions are amplification and amplitude, which change the balance between frequency and wavelength of the optical signal. Consequently, the filter will need to be readjusted if either of these two factors changes [37].

Also in Figure 3.7, it is used four channels to transmit information, a Red, Green, Blue and Violet LED, each with its own specific bit sequence. Each channel has a different wavelength, so when the channels are mixed together, they are absorbed

in different areas of the receiver. An analysis of this received signal is conducted by measuring the generated photocurrent under an applied voltage of -8 V and a background light of 390 nm [37].

To decode the MUX signal, an algorithm is needed. The background acts as a selector that picks one of the 2^n, where n is the number of transmitted channels. The levels in the MUX signal differ for each of the possible 2^n states. If all channels are present, there will be 2^n levels, each with its own optical gain. Using a five channel transmission [37], it is possible to decode the signal at 60 kbps using n binary codes assigned to each level.

The proximity of consecutive magnitude levels can cause errors when decoding the levels. By using parity bias control, this problem can be solved. By calculating the code from the incoming bits and comparing it to the incoming code, the receiver checks for errors [37].

4

Simulation

The purpose of this chapter is to simulate the proposed scenario, described in chapter 3, using a simulation tool named Zemax Opticstudio. In order to compare and analyze them with the proposed work explained earlier, it will be briefly explained how the tool works, what components were used, and what results were obtained [38] [39] [40].

4.1 Introducing OpticStudio

Zemax OpticStudio, is an optical simulation tool that can model various optical prototypes and create optical system scenarios. By using this software it was possible to build the scenario discussed in chapter 3 and simulate it. For an accurate explanation of the results and scenarios obtained, some elements of the software must be explained.

In this section, a brief introduction about OpticStudio is made, as well as some of its features by building a simple scenario, that allows to explore this tool and learn how to use it. First by starting to show the interface in Figure 4.1.

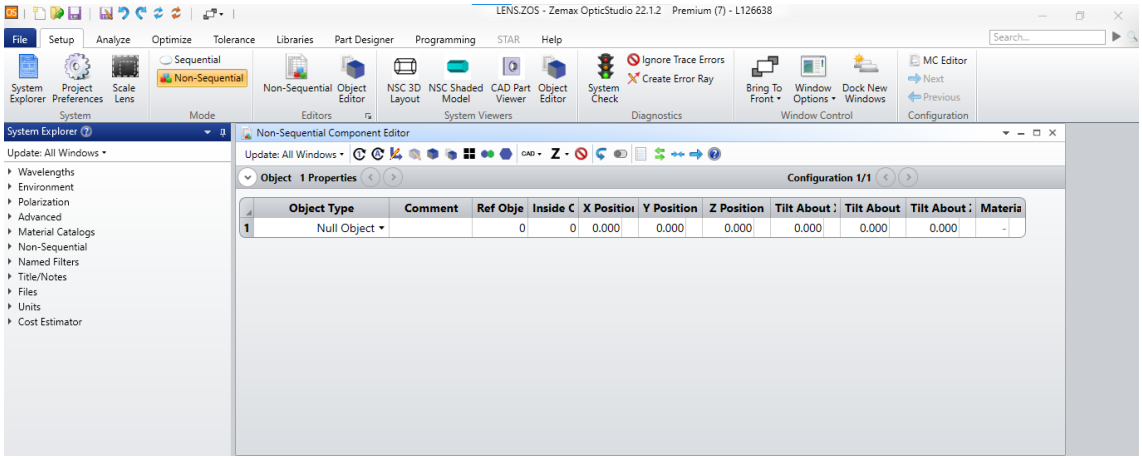

Figure 4.1: OpticStudio's interface.

In Figure 4.1, you can see what the initial software interface looks like. Initially, a single LED and detector was used to illustrate how components are placed and manipulated to create the desired scenario.

4.1.1 Optical Source

As a first step, it is necessary to have a light source along with a detector. To add a light source, extend the object properties and select sources under the general category. A variety of light sources are available in the types options, but for this example, a source point was used. This option is highlighted in Figure 4.2. It is important to note that all of this scenario building and the measurements are done in non-Sequential mode, which is also highlighted in the Figure 4.2.

Each object in this software has its own parameters, which can be changed to affect the result or scenario. In regards to source objects, the first five parameters are the same for all of them, and in this case, the source point has a sixth parameter. They are as follows:

1. # Layout Rays: When creating layout plots, this determines how many random rays to launch from the source. Only the scenario, or layout, shows this number of rays.

2. # Analysis Rays: When performing analysis, this parameter specifies how many random rays to launch from the source. The number describes how many rays the source emits, and can only affect the final results; it cannot be seen on the layout.

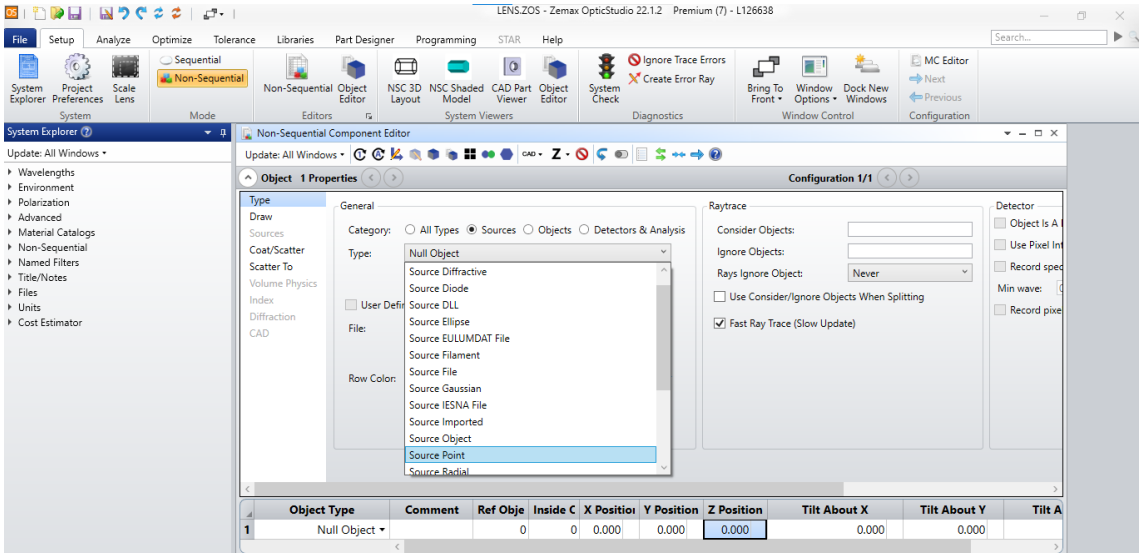

Figure 4.2: Source point Option.

3. Power (units): Over the defined range of the source, this is the total power. Therefore, if the power is set to 1 W, the total power captured will be 1 W, regardless of distance. Watt, Joule, or Lumen can be defined as the source unit.

4. Wavenumber: The wavenumber to use when tracing random rays. Therefore, changing the wavenumber will alter the wavelength, since the wavenumber matches a certain wavelength. Later, it will be shown how to set and change wavelengths on source objects.

5. Color #: This parameter changes the rays' color. In the case of zero, the default color will be used. Later on, it will be shown how to view the color corresponding to the wavelength.

6. Cone angle: The semi-cone angle in degrees. This parameter allows to adjust the beam angle. The cone angle may be any value between 0 and 180 degrees, which would radiate into a full sphere.

Another source object worth mentioning, is a source file. The Source File is a source whose ray coordinates, cosines, and intensity are defined in a user supplied file. Radiant source models can be downloaded using OpticStudio software, and in order to use these sources, it is necessary to select source file, under the source option, shown in Figure 4.2. The source file shares the same first five parameters mentioned earlier. The Figure 4.3 depicts this choice.

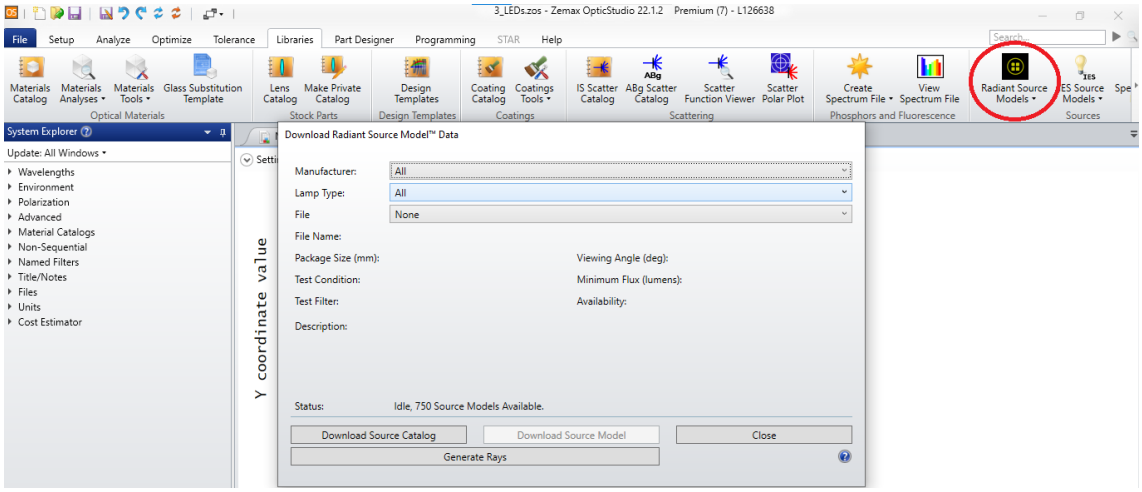

Figure 4.3: Radiant source models.

It is possible to select the desired LED or other type of source from an existing manufacturer of light sources using the option highlighted in Figure 4.3. To utilize it in the suggested situation, its attributes and file name are shown below in the window. With the chosen light source, it is possible to plot the directivity of the LED and also the polar plot. The Figure 4.4 show the directivity plot and polar plot, respectively, using a green CREE manufactured LED.

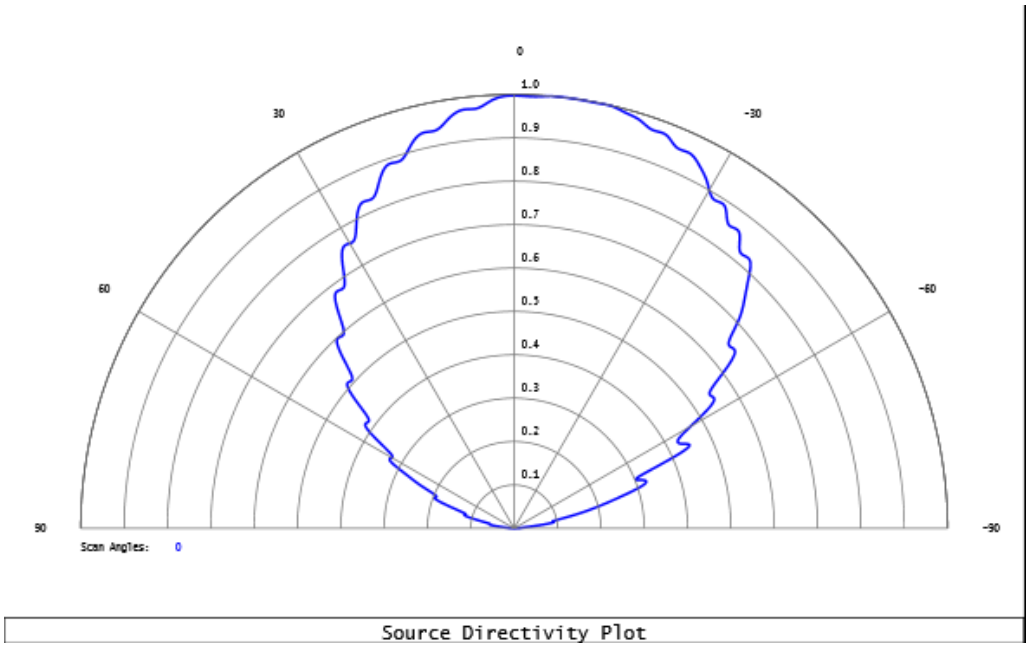

Figure 4.4: Directivity plot of a green CREE LED.

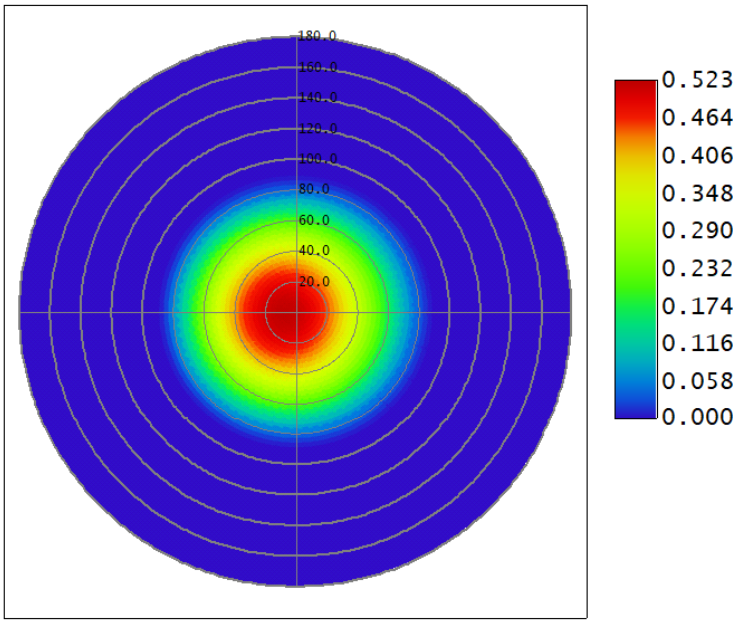

Figure 4.5: Polar plot of a green CREE LED.

An example of another source object that can be used is a Source Filament. The Source Filament can be thought of as a thin wire coiled in a helix shape. The wire turns "N" times along the full Z coordinate length given by "L". The radius of the turns is defined by "R". Rays emanate from a randomly chosen point along the helix in a random direction. The filament share the same first five parameters mentioned before, and has three more parameters that can be changed, these are:

6 Length "L" in lens units. This alters the length of the filament. Lens units are the primary unit of measure for the lens system. Lens units apply to radii, thicknesses, apertures, and other quantities, and may be millimeters, centimeters, inches, or meters.

7 Radius "R" in lens units. This parameter changes the radius of the turns.

8 Number of turns "N" (dimensionless). N may be fractional or even negative to reverse the rotation direction of the helix.

An example of a filament in OpticStudio can be seen in the Figure 4.6.

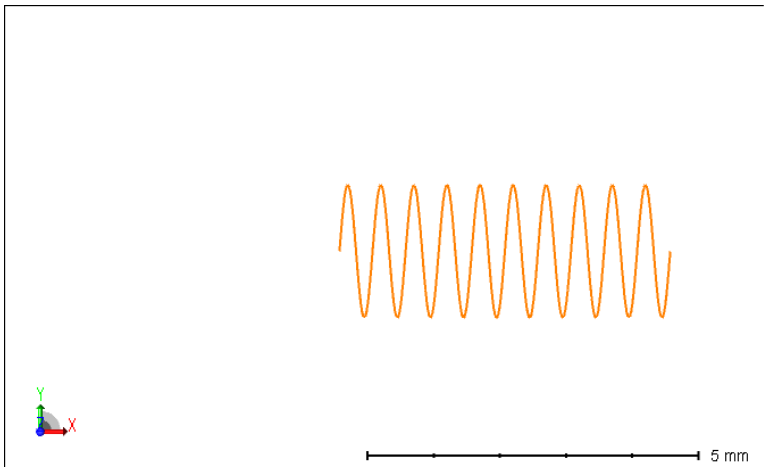

Figure 4.6: Example of a filament in OpticStudio.

Many more source objects are available in OpticStudio, all of which have their own purpose and parameters. Source point source object was used in this example to demonstrate how the software works. As mentioned earlier, one of its parameters can change the wavelength of the source.

It takes two steps to change the wavelength. On the software's interface, select the wavelength option and change the wavelength value. In this example, the wavelength used was 700 nm. This is shown in Figure 4.7.

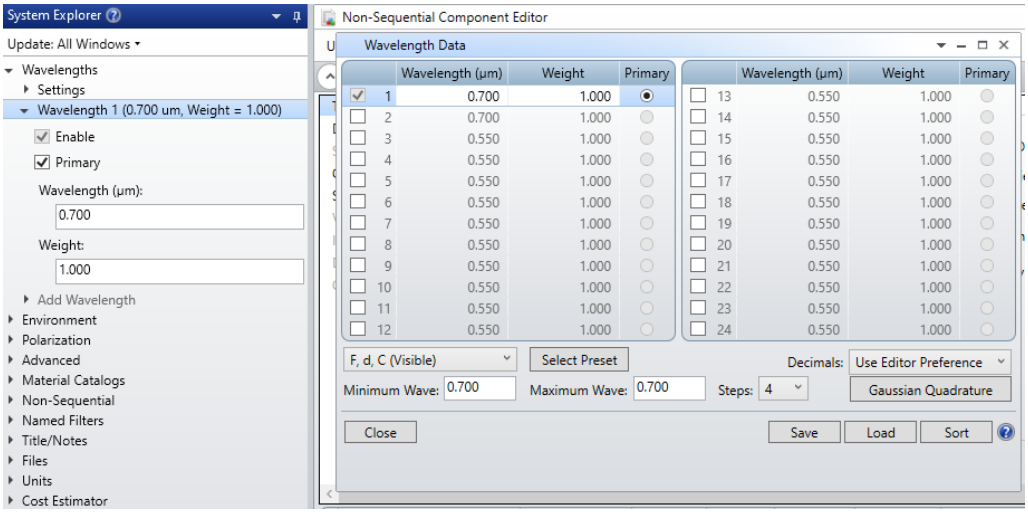

Figure 4.7: Adding wavelength.

Next, we must change our source point to the wavelength we just created. In order to change the wavelength of our source point, we must go to the wavenumber parameter of object 1, since this is our source point. The Figure 4.8 illustrates this.

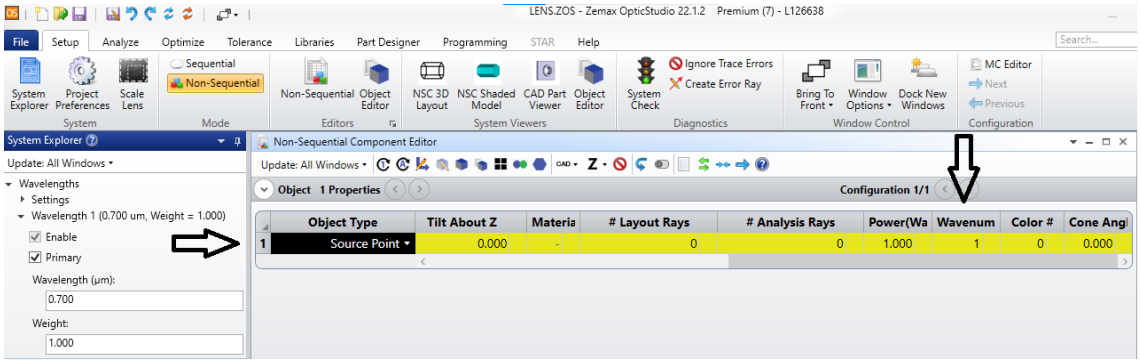

Figure 4.8: Changing the source's wavelength.

In Figure 4.8, an arrow indicates the parameters, including the wavenumber parameter, which is set to 1. The wavelength we created has the same number, which can be seen again in 4.7. When we set this parameter to the wavelength number we want, the wavelength of the source point is now changed.

If there are multiple source objects with different wavelengths, as in this work, it is possible to have multiple wavelength numbers active.

4.1.2 Detector

Before any parameters are changed, a detector is needed. To add a detector, it is necessary to add another object, which is done by going to the object editor and using the right click of the mouse, this will open a window of options, and after selecting 'insert object after' the object is added. This can be visualized in Figure 4.9.

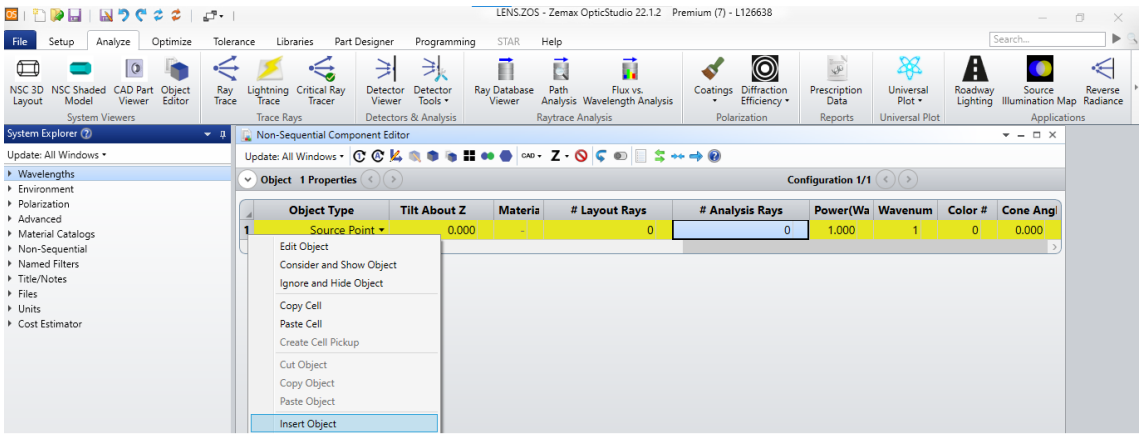

Figure 4.9: Inserting an object.

We now have two objects after selecting the correct option. Object 1 remains our source point, and object 2 needs to be defined. Therefore, to change our object 2

into a detector, we need to open its properties, select 'Detector & Analysis' in the category options, and then choose 'Detector Rectangle' for the type of detector. The Figure 4.10 highlights these options.

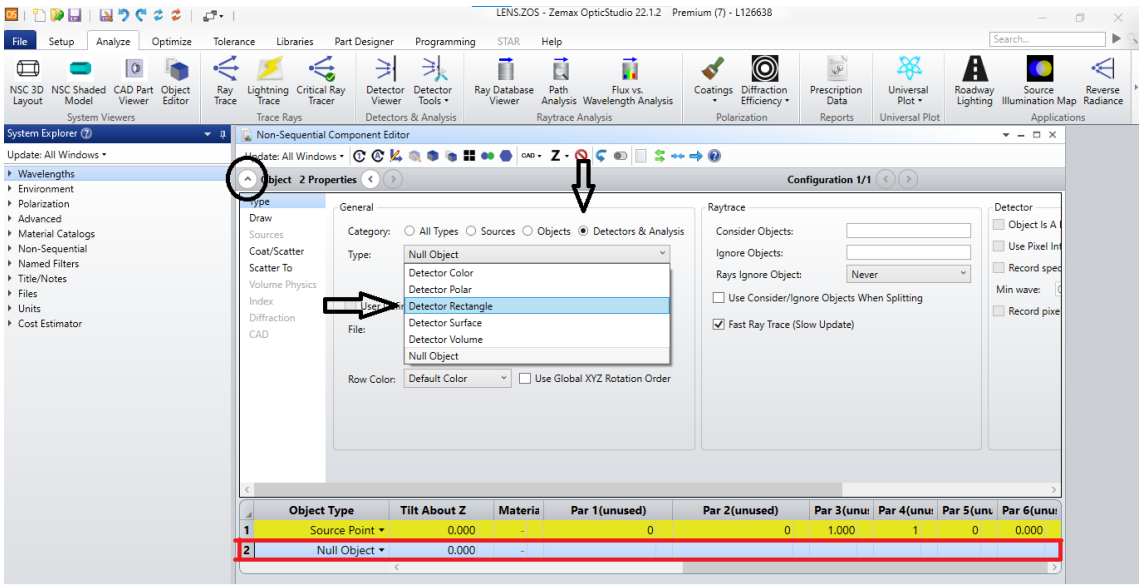

Figure 4.10: Changing object to detector.

Figure 4.10 shows several detectors that can be selected. Two detectors were primarily used throughout this work, one of which was the detector rectangle.

In this software, a detector stores energy data from rays that strike them. Detectors can be reflective, transparent, or absorbing. In this case, the detector is set to absorb the rays.

For every ray that strikes the detector, four data items are captured. The incoherent intensity of the ray, as well as the intensity of the ray in angular space. Moreover, it can store the combined intensity of the ray divided by the area of the detector's pixels. In addition, it can store its combined intensity divided by the angle of the ray.

The electric field of each ray can be written as:

$$E_n = A_n\, e^{i\varphi} = A_n\, \cos\varphi_n + iA_n\, \sin\varphi_n \tag{4.1}$$

Where A_n is the amplitude and φ_n is the phase.

The detector has four defining parameters, and these are:

1 X Half Width. The x width in lens units.

2 Y Half Width. The y width in lens units.

3 # X Pixels. The number of pixels along the x direction.

4 # Y Pixels. The number of pixels along the y direction.

The rest of the parameters are only used to define how the detector is displayed on shaded model plots. These will not influence the experimental results.

The other type of detector used is the detector color, this object stores power and tristimulus (visual light color) data from the simulation performed. The resulting data distributions may be viewed for incoherent light in spatial or angular domains. The defining parameters for this detector are the same as the rectangle detector mentioned before.

It is necessary to change some parameters on both objects before viewing the layout. The parameter 'Layouts Rays' was set to 50 after selecting the source point object. When creating layout plots, this specifies how many random rays should be launched from the source. These rays will be visible later. To obtain a large sample of light, the parameter 'Analysis Rays' will be set to one million. This parameter determines how many random rays to launch from the source when performing analysis. The power of the source point is left by default at 1 W. Next the Z position was set to 20, which is moving the object 20 mm in the Z axis, and in the parameter 'Tilt about Y' was changed to 180º, in order to face the LED down. Lastly, the parameter 'Cone angle' was set to 50º. These changes can be seen in Figure 4.11.

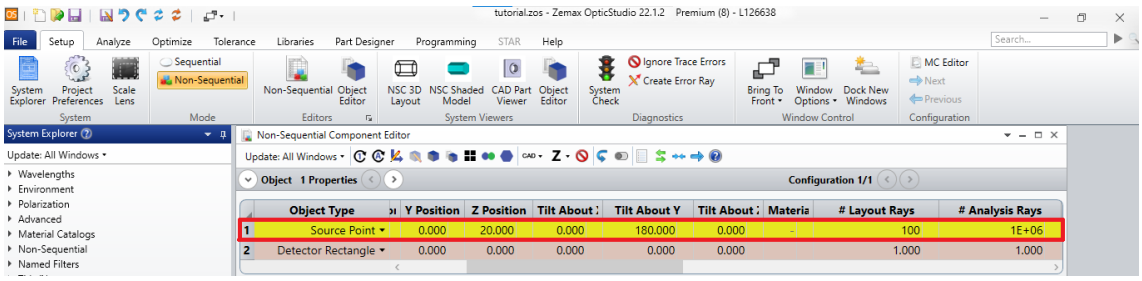

Figure 4.11: Changing parameters of the source point.

For the detector, both the 'X Half Width' and the 'Y Half Width' parameters were set to 30, which corresponds to the detector size, 30x30 mm in this case. In addition, '# X Pixels' and '# Y Pixels', both of which define the number of pixels in each direction. The Figure 4.12 shows the final parameter changes.

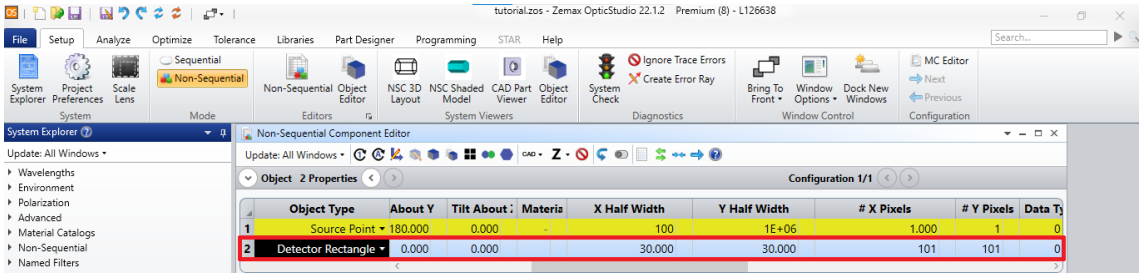

Figure 4.12: Changing parameters of the detector.

4.1.3 Scenario definition

The created scenario can now be visualized after all these changes have been made. You can do this by selecting the 'Analyze' tab and selecting 'NSC 3D Layout'. The highlighted options can be seen on Figure 4.13.

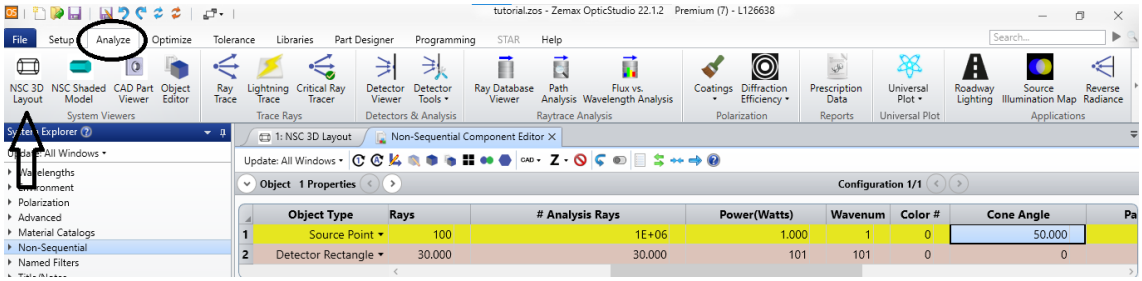

Figure 4.13: NSC option.

And after selecting this option, the scenario obtained is shown in Figure 4.14.

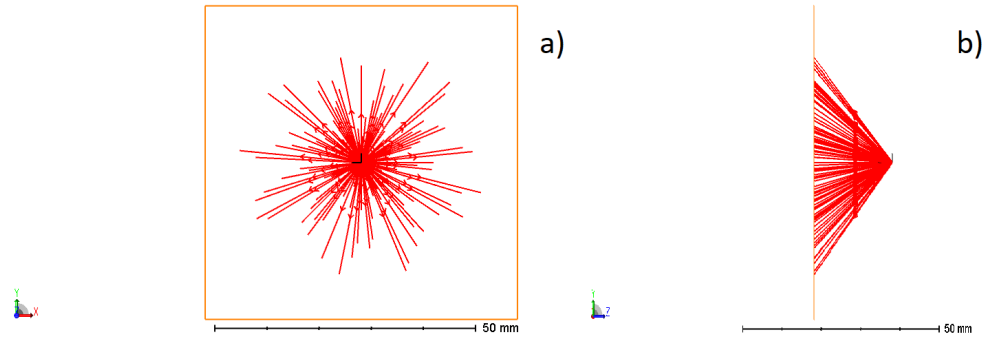

Figure 4.14: (a) Top view of the LED and detector (b) side view of the LED and detector.

In Figure 4.14 it is shown a red LED with a wavelength of 700 nm, emitting light directly to a detector. Users can modify the scenario in any way they like. To accomplish this, you can either change the coordinates of the objects or simply add more to the scenario. When viewing the 3D layout, it is necessary to change the 'Ray Trace' option under the settings option to 'Use rays' in order to view the correct number of rays.

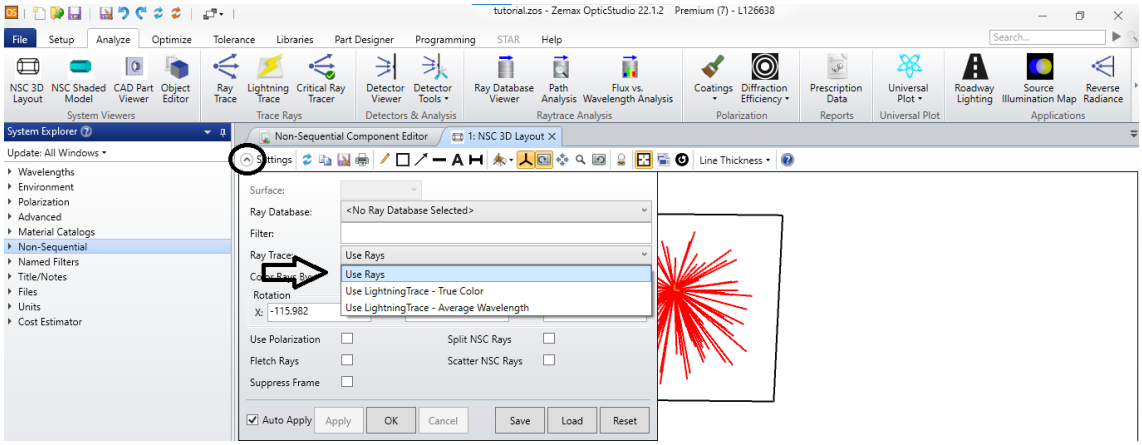

Figure 4.15: Option to view the layout rays.

The detector must be simulated in order to see what it is capturing, as shown in Figure 4.16 and Figure 4.17.

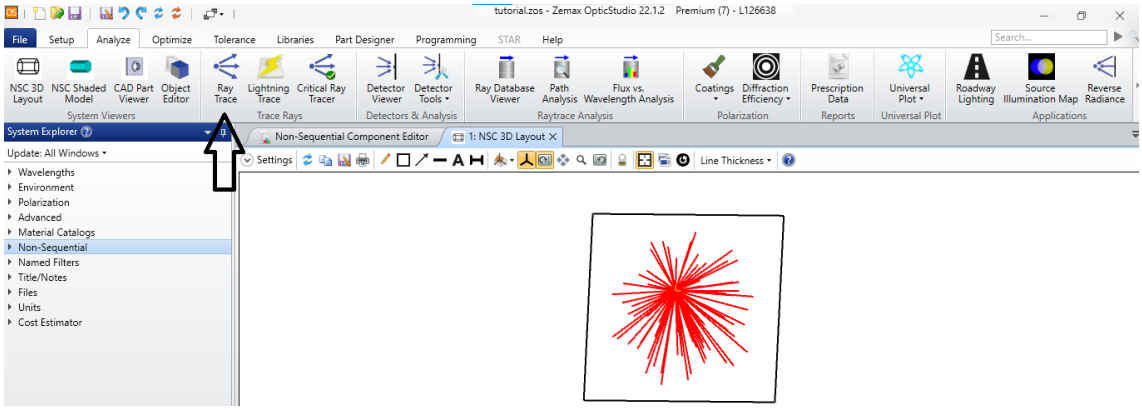

Figure 4.16: Ray trace option.

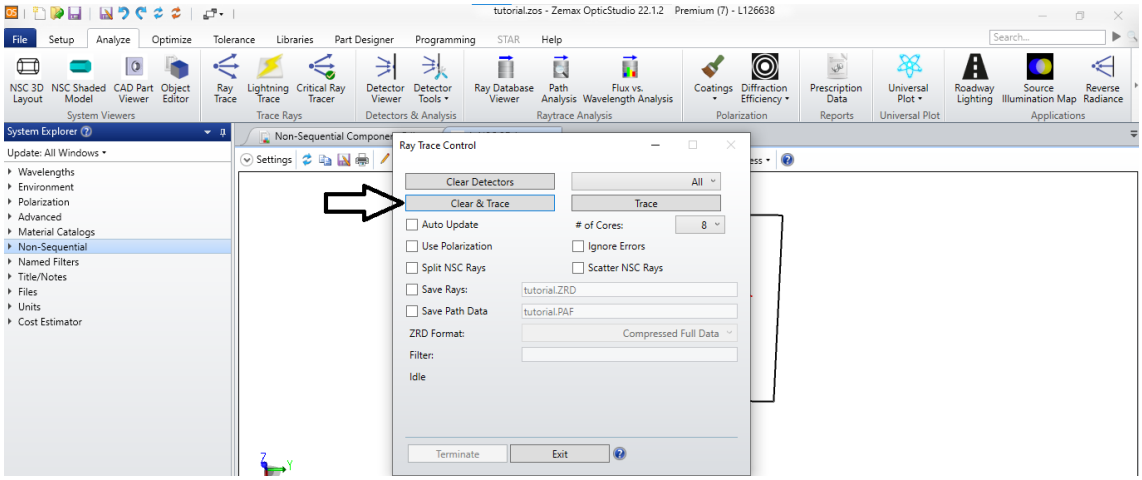

Figure 4.17: Clear & trace option to begin the simulation.

Upon selecting these options and waiting for the simulation to run, the rays have been traced, and the detector can now be viewed to see what has been captured. In the 'Analyze' tab, the 'Detector View' option allows the user to view the simulation results.

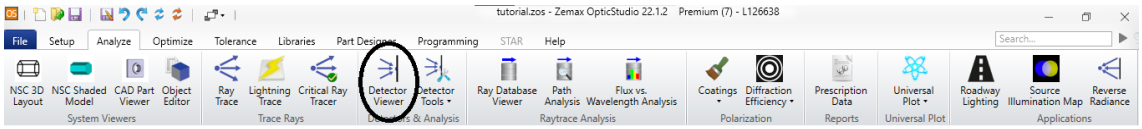

Figure 4.18: Detector view option.

The results of this first scenario are shown in Figure 4.19.

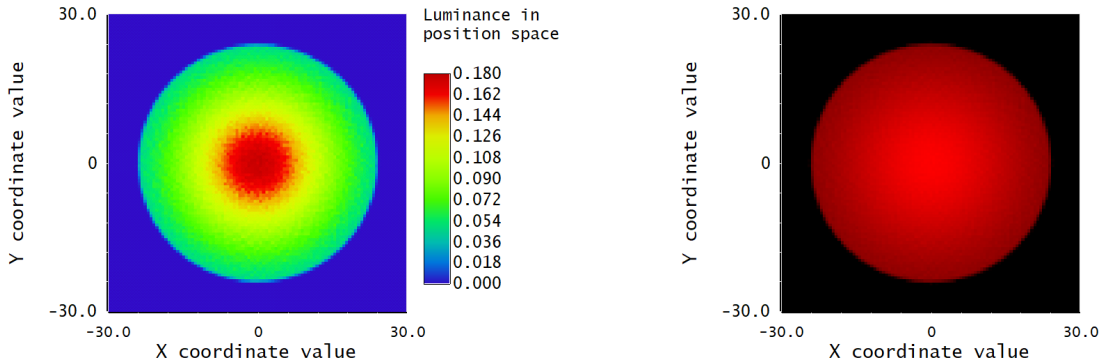

Figure 4.19: Light and colour captured with detector.

In order to obtain color, a color detector is needed, which is an option on detector types. This result was achieved by adding a color detector in place of the regular detector, just to capture the color. To achieve these results, we used the settings in Figure 4.20 on the rectangle detector.

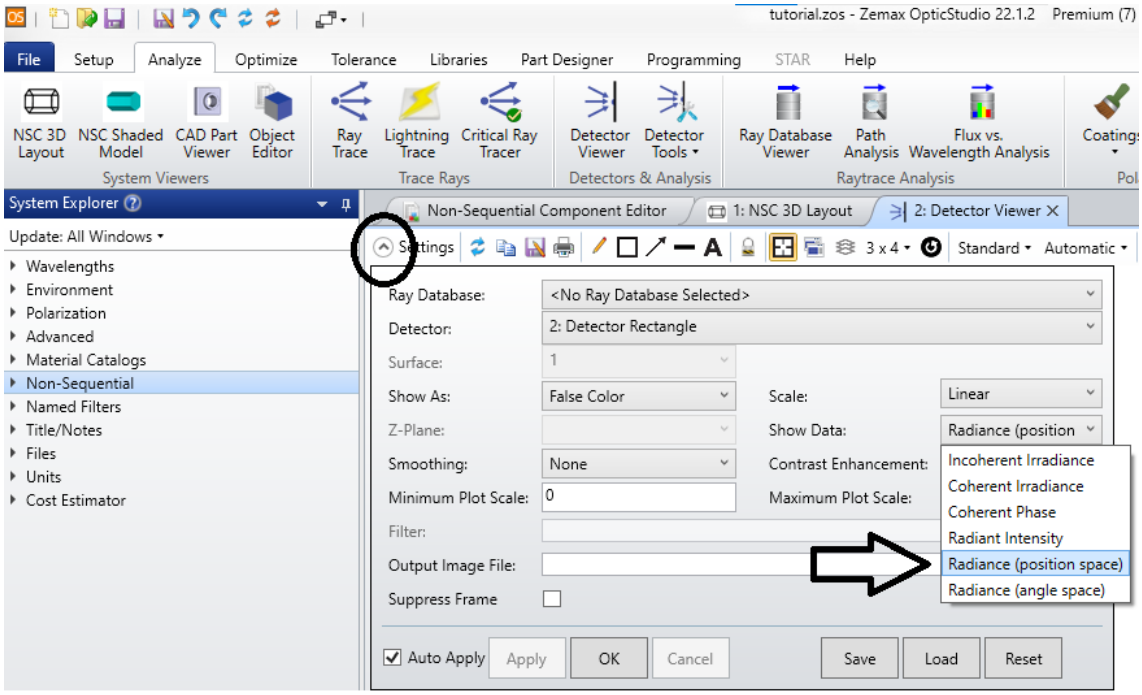

Figure 4.20: Settings used for the regular detector.

And for the color detector, these settings were used.

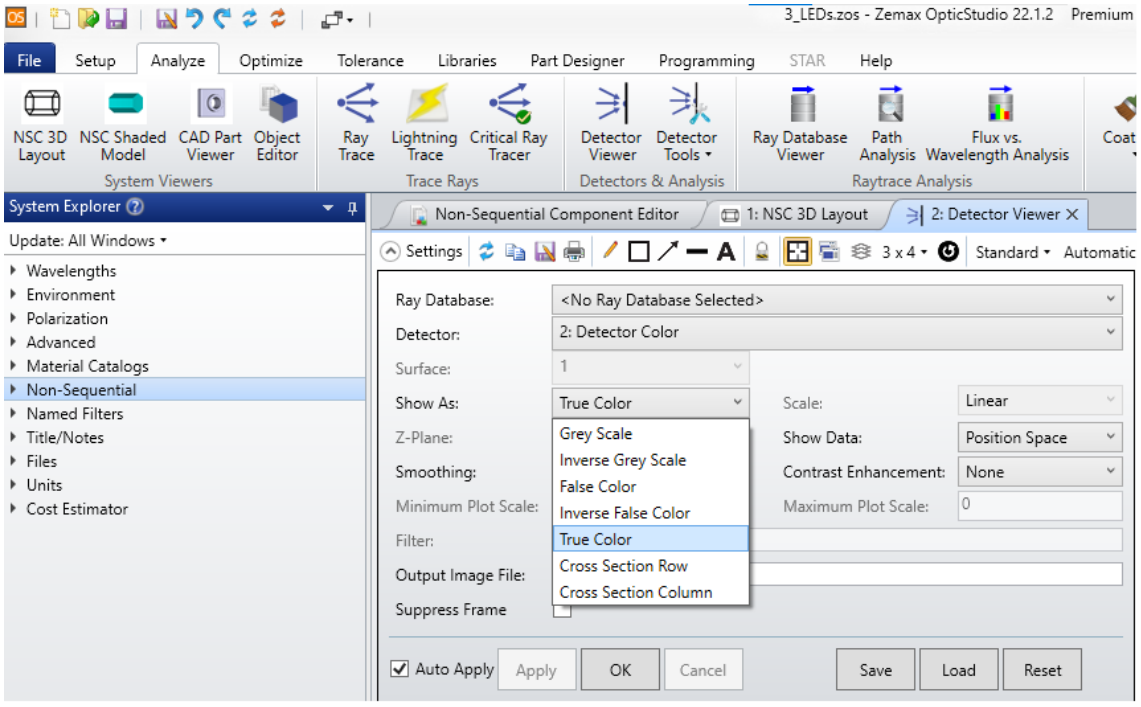

Figure 4.21: Settings used for the color detector.

It is important to note that, when using more than one detector, it can be selected which detector to show results. This option is on settings next to 'Detector'. This

option can be viewed in both Figure 4.20 and Figure 4.21.

Figure 4.19 shows LED light intensity and color, and since the wavelength is 700 nm, the color is red. It is expected that the intensity graph is more intense at the center of the detector, since the LED is radiating there, and that it is lower away from the center.

After completing the first scenario, the basic of this software are now known. There are no objects in this built scenario; the source emits directly into the detector in line of sight. In a real-world application, there are many objects, such as buildings, that can reflect some light, especially if they are made of metal or glass.

4.1.4 Non Line of sight conditions

One way to simulate this situation is to add some surrounding objects and make them reflective and test how it changes the results. This effect is exemplified in Figure 4.22. In this new scenario, the green car emits light directly to the red car, establishing a communication link. The red car is equipped with a detector at the rear. In addition, two reflective objects were placed on either side of the green car, one to the left and one to the right.

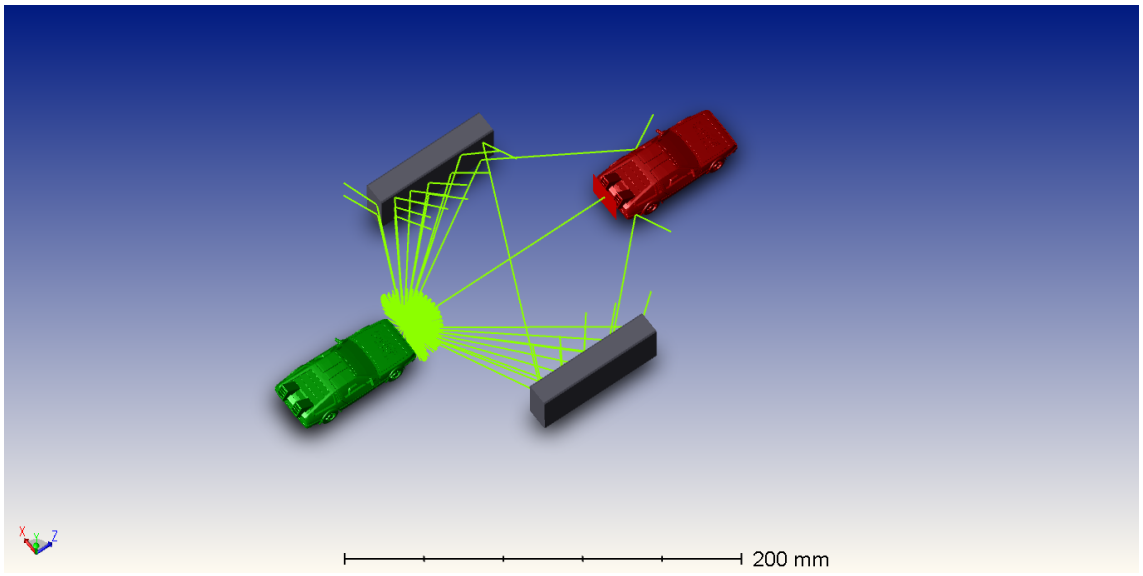

Figure 4.22: Reflective effect in OpticStudio.

It can be seen in the last figure that the red car, which is equipped with a detector at the rear, emits light, while the green car emits light. Using these two reflective blocks, the green car's light is reflected back to the red car at a different angle.

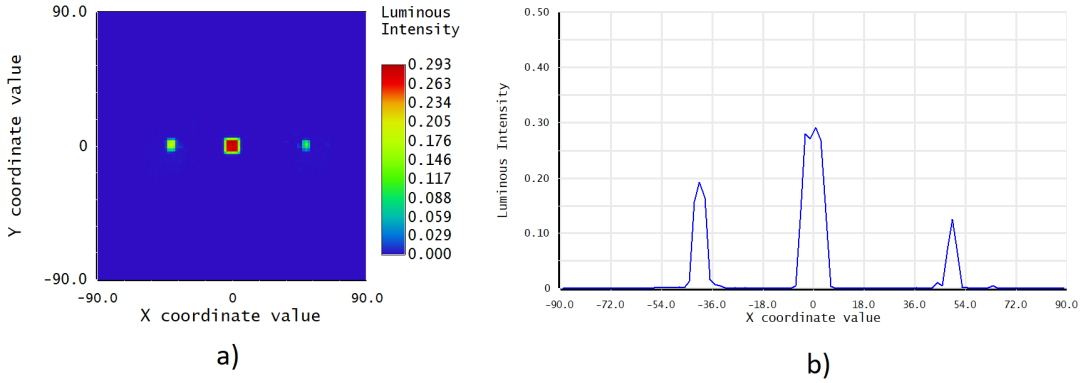

Figure 4.23: Reflected light in OpticStudio.

Light is most concentrated in three different spots. Figure.4.23.b) shows the line of sight, which is directly emitted to the detector, and two other spots that are reflected from the blocks at an angle.

The Figure 4.24 shows how to setup a reflective object.

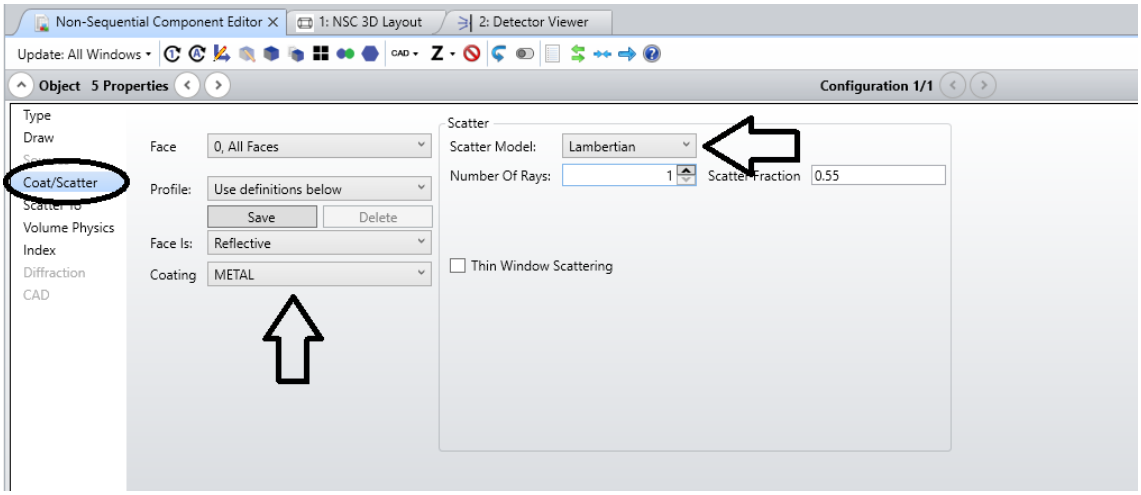

Figure 4.24: How to setup a reflective object.

On the example, the reflective blocks are also shown with their options. After choosing the reflective option, a metal coating was applied to the objects, and the lambertian scatter model was used.

For lambertian scatter, the scattered ray projection vector has equal probability anywhere on the projected plane. This results in a scattered intensity variation of the form $\cos(\vartheta s)$. The scattered intensity is independent of the incident angle.

The Bidirectional scattering distribution function (BSDF) is $1/pi$.

4.2 Simulation Results

The first step to replicate the proposed work discussed in Chapter 3, is to recreate the footprint of the intersection. It was accomplished by using four LEDs placed at the corners of a square configuration as shown in Figure 4.25.

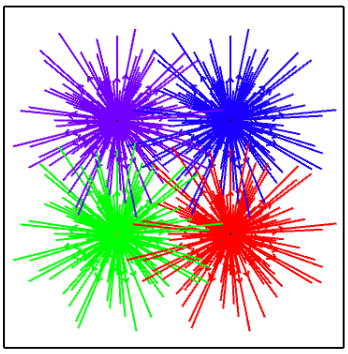

Figure 4.25: Four LEDs to create the footprint.

It is possible to recreate a footprint using the four LEDs as illustrated in Figure 4.25; this footprint will be placed at the intersection to create the proposed scenario based on the configuration presented in Figure 4.25. To cover the footprint, we used a red LED powered by 4 W at 700 nm wavelength, a green LED powered by 3.75 W at 550 nm wavelength, a blue LED powered by 3 W at 460 nm, and a violet LED powered by 2.25 W at 390 nm wavelength. The cone angle of all LEDs is 50 degrees. The footprint is shown in Figure 4.26.

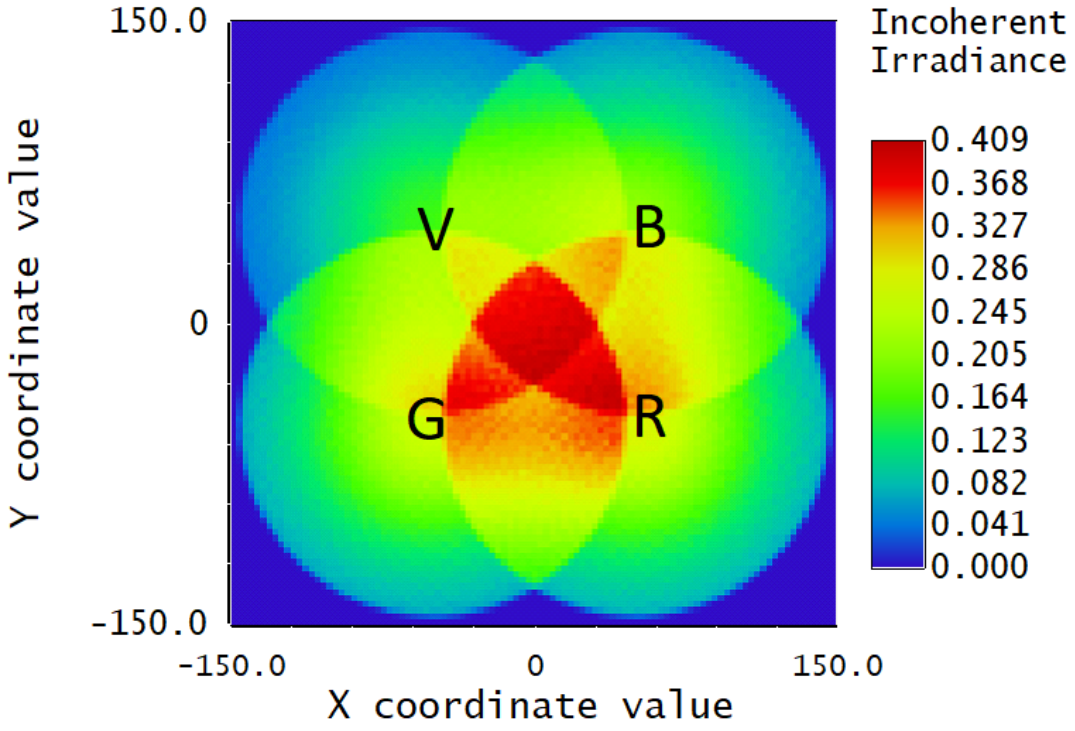

Figure 4.26: The footprint obtained with the regular detector.

In Figure 4.26 it is shown what the detector captures in all of its position in space. However, the desired footprints are focused in the middle of the detector, where the irradiance values are higher, caused by the overlap of the LEDs.

It is possible to switch the detector to a color detector to view the overlapping of the channels. This can be viewed in Figure 4.27.

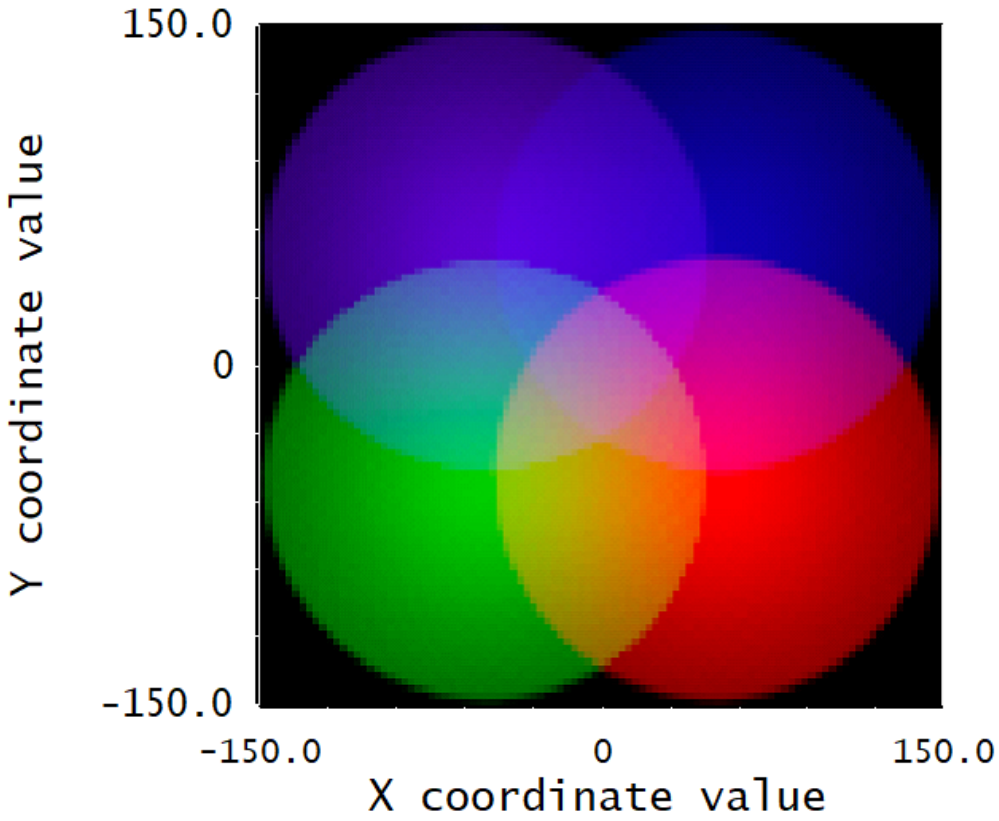

Figure 4.27: Footprint using a color detector.

It is possible to see the channel overlap and the actual mixing of colors that the combinations result in Figure 4.27.

However, the detector's center must be improved in order to see the true footprint. Therefore, employing a regular detector once more and after boosting the footprint, the enhanced footprint is shown in Figure 4.28, with each position identified with its respective overlapping channel.

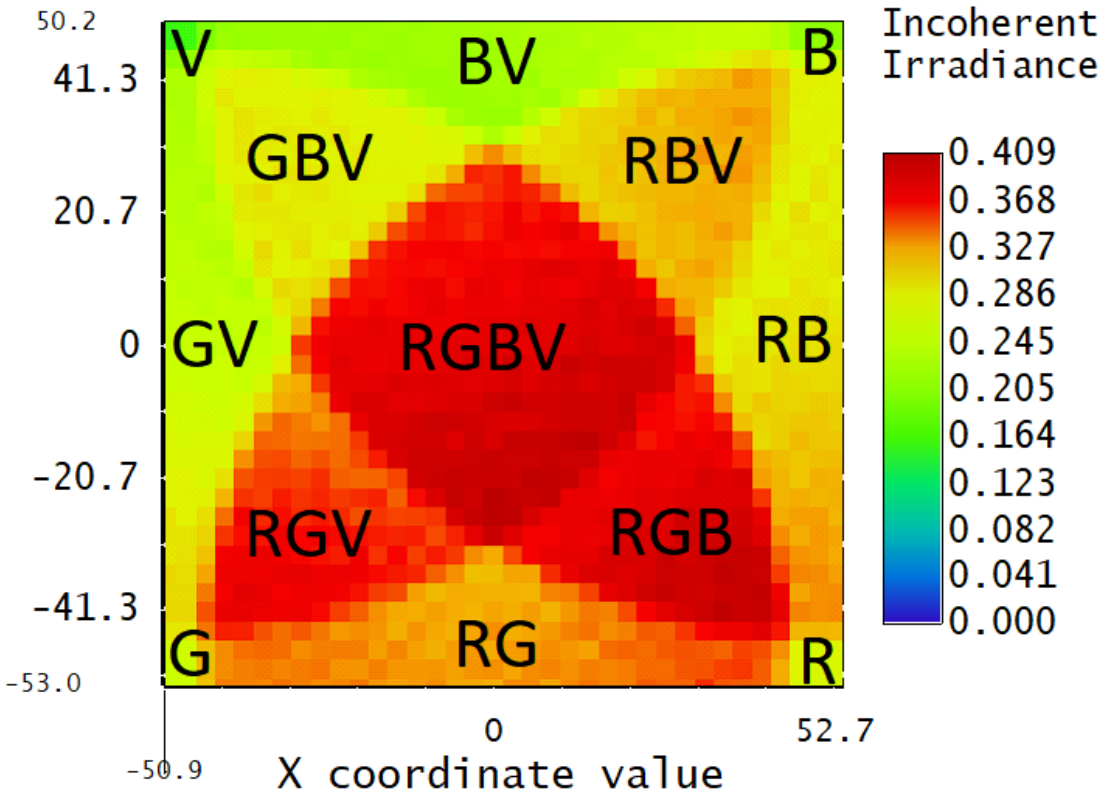

Figure 4.28: Enhanced footprint.

In Figure 4.28, the nine different footprints are shown, which correspond to the nine positions that the four LEDs can take. It can also be seen that the intensity level of each position corresponds to the intensity level of the calibration of the proposed work. The calibration signal can be viewed in Figure 4.29.

Red LEDs are more intense, while violet LEDs are less intense, in order to produce the right calibration curve, in [15].

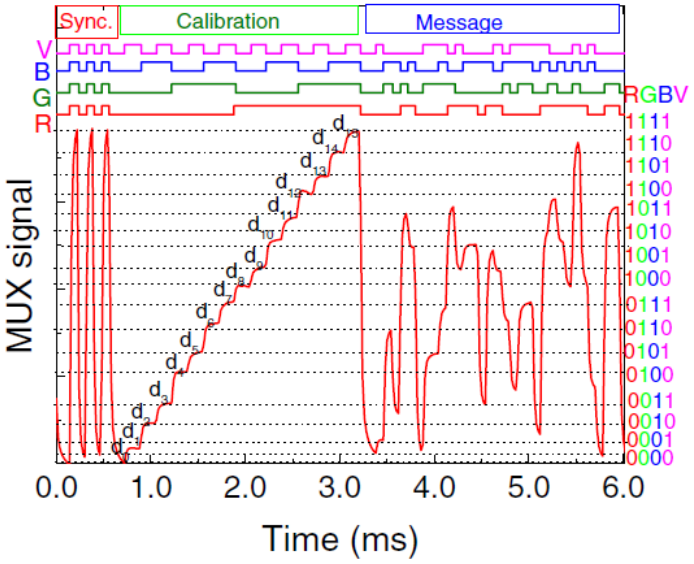

Figure 4.29: The MUX/DEMUX signal of the calibrated cell [15].

If we compare the intensity levels of Figure 4.29 and Figure 4.28, we can conclude that it matches. Since the LEDs have different powers, the nine different footprints have different intensity levels. Thus, the intensity levels obtained in the software match those in [15]. Consequently, the powers used in the software are correct for the proposed work. The center footprint is the most intense, as it contains all four channels, so it is RGBV. The next level of intensity is RGB, up until the last level of intensity, which is all channels off.

With the footprint done, it must be applied to the proposed intersection. In order to do that, it was exported a 3D model of an intersection to OpticStudio, to make the scenario more clear. The intersection used can be seen in Figure 4.30.

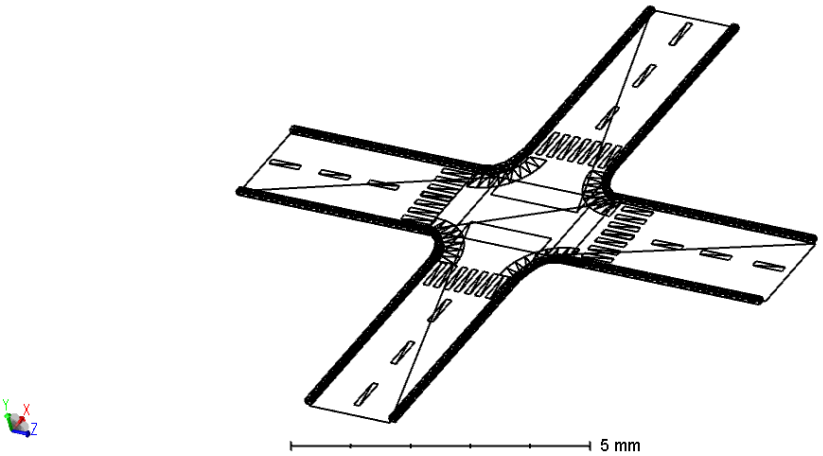

Figure 4.30: Intersection used for simulation

Once the intersection model has been imported, the LEDs need to be inserted. Following exactly the same scheme as in Figure 3.2, this procedure was carried out.

In order to complete this scenario, light posts and traffic lights were added to create a simulated street. The completed scenario can be seen in Figure 4.31.

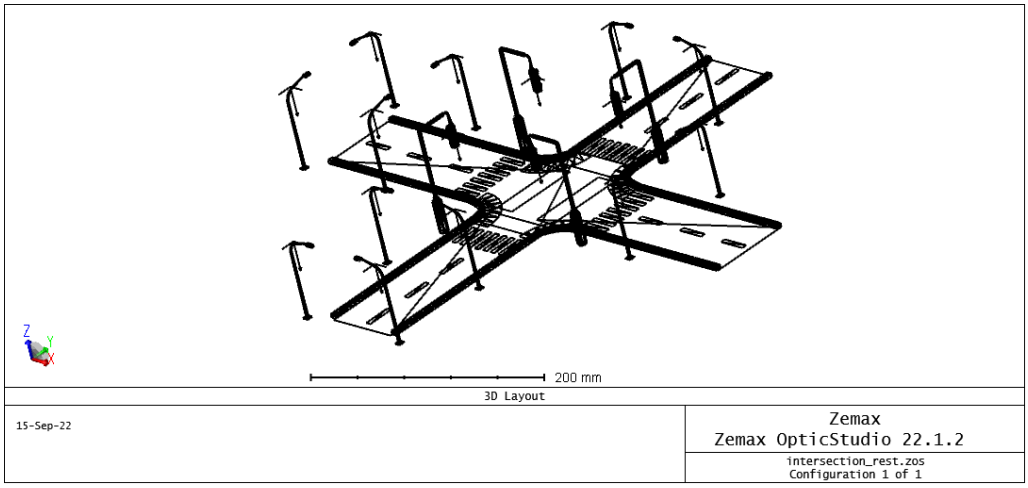

Figure 4.31: Intersection scenario without LEDs

It is now possible to see where the LEDs will be placed. Accordingly, LEDs were inserted in the correct positions following the proposed work scenario.

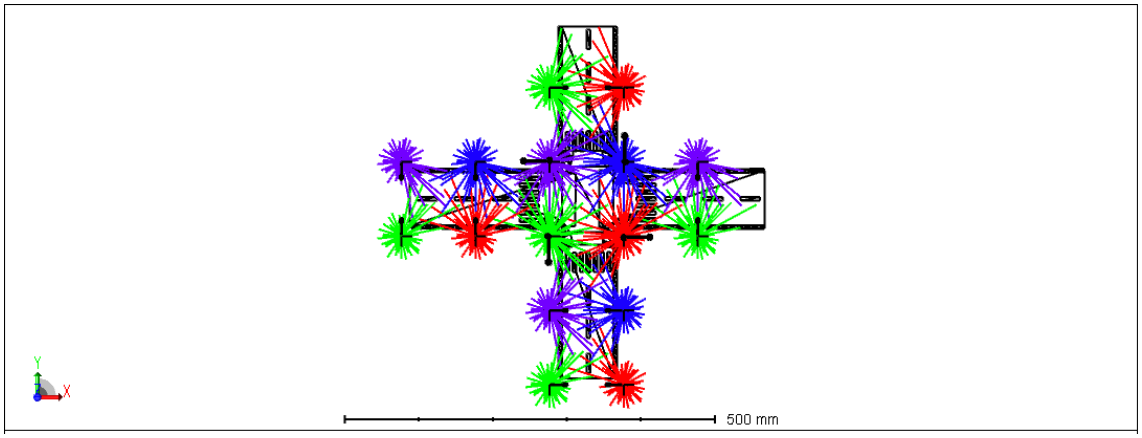

Figure 4.32: Intersection simulation

With the LEDs placed, it is now possible to trace the intersection footprint map.

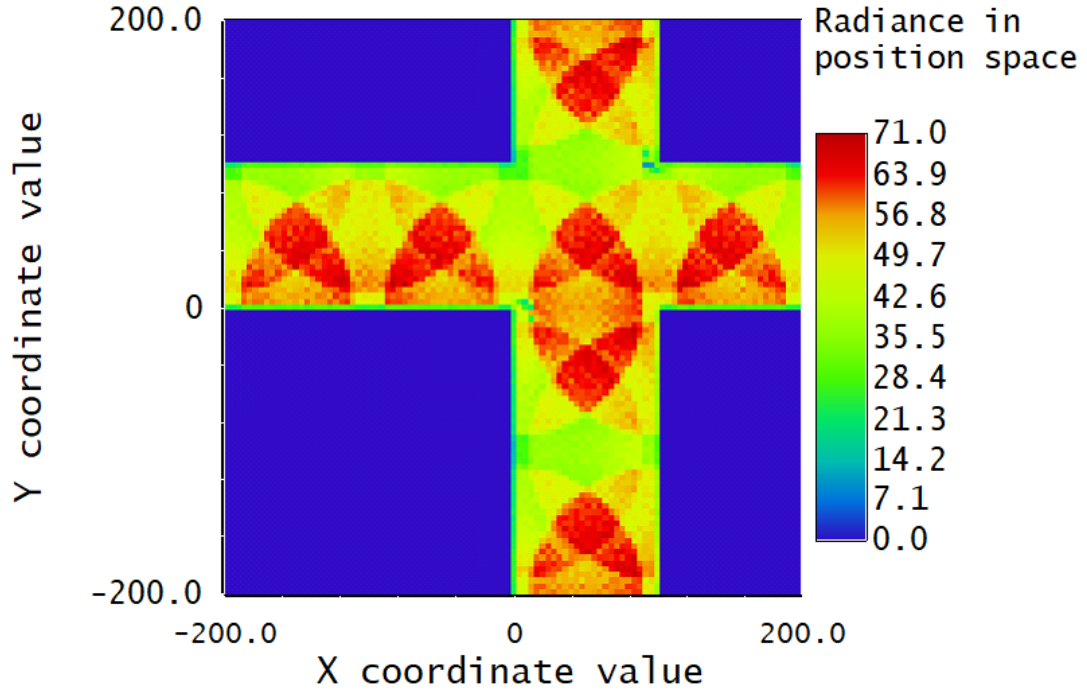

Figure 4.33: Intersection footprint

With the Figure 4.33, it is possible to now compare the scenario with the proposed work scenario, in Figure 3.2.

Every position in the intersection can be seen in this Figure 4.33. Because a vehicle passes through multiple footprints during a maneuver, based on the unique ID of each LED and the angle the vehicle is making, it is possible to know every position the vehicle is making throughout the intersection. Additionally, it shows what the detector on the car captures depending on its position in the intersection.

A color detector can also be used to view intersection footprints from a different perspective.

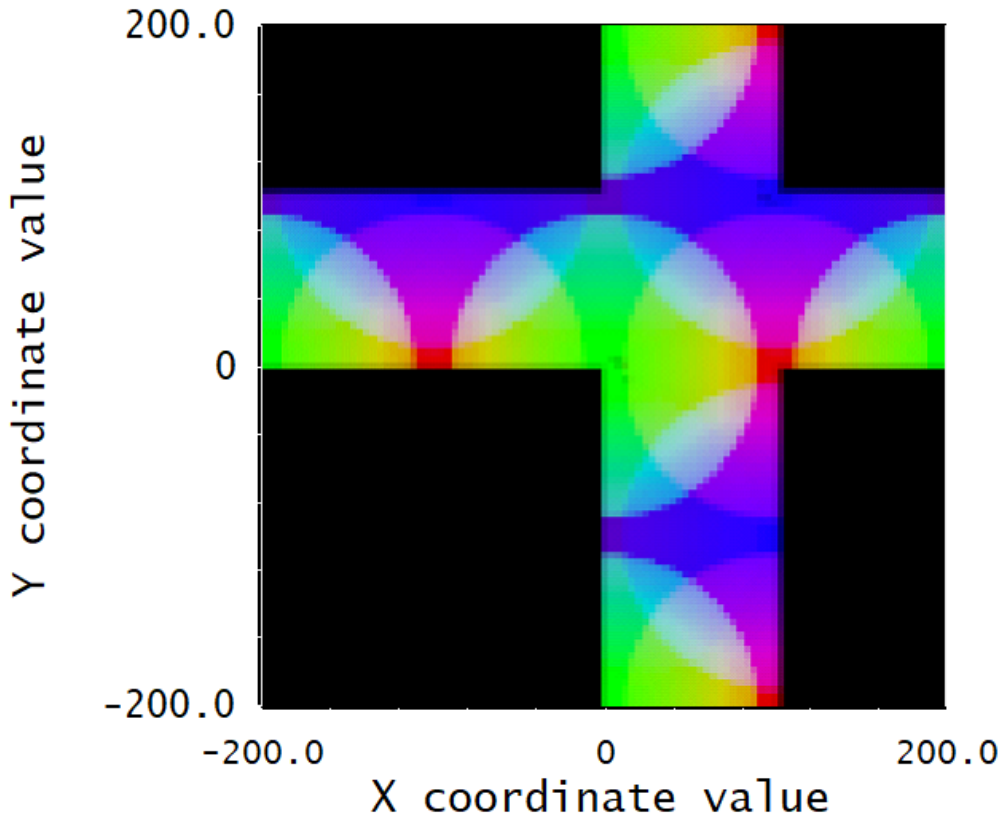

Figure 4.34: Intersection footprints using a color detector

After switching to a color detector, it is possible to view the actual position of each channel in the intersection and its range.

5

Experimental Results

The purpose of this chapter is to present a test scenario in which a vehicle makes a specific trajectory and passes through cells of intersection footprints. An illustration will be provided of the vehicle's maneuver, as well as the information it sends regarding its position in the intersection.

These results were taken in lab, due to the limitations of the software used in Chapter 4. At the time of this work, this software cannot modulate light sources in order to send information.

5.1 Footprint Map

As explained in Chapter 3 and simulated in Chapter 4, the footprint map represents the overlap of LED transmission ranges. A footprint obtained from the software, with each position numbered, is shown in the Figure 5.1.

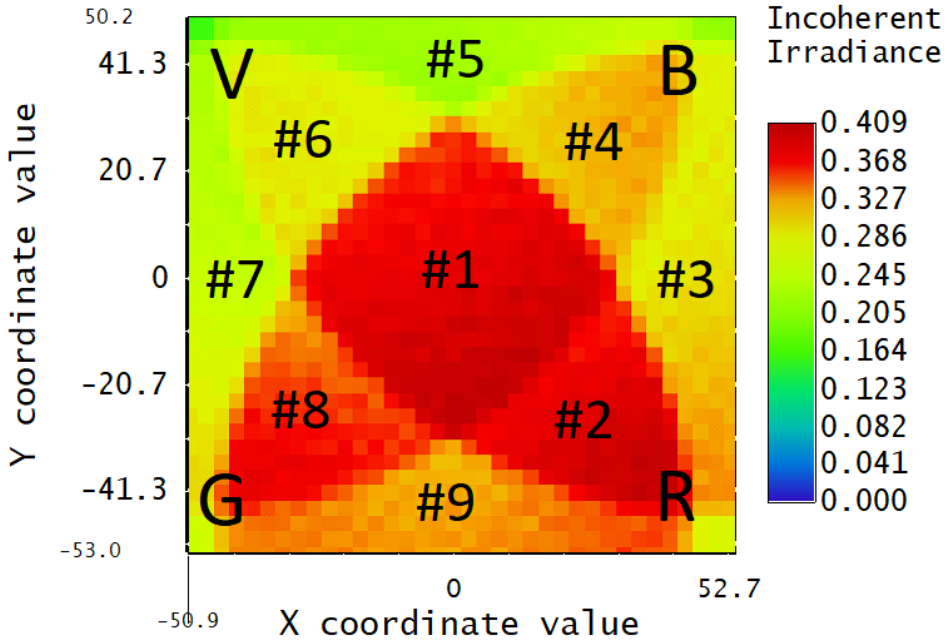

Figure 5.1: Footprint map of one cell.

This Figure shows the overlap of the four LEDs in the center as the footprint #1. The adjacent footprints #2, #4, #6 and #8 have three channels overlapped. Finally, the footprints #3, #5, #7, and #9 have only two overlapping channels at the top, bottom, left, and right.

5.2 Lab Software

The lab results were obtained using software called 'PiscaLed'. With this program, you can select from a variety of synchronous on/off patterns with fixed individual currents for 16 LEDs. Fixed LEDs shine directly onto an optical sensor, namely the same receiver as described in Chapter 3. An example of the program's interface can be seen in Figure 5.2.

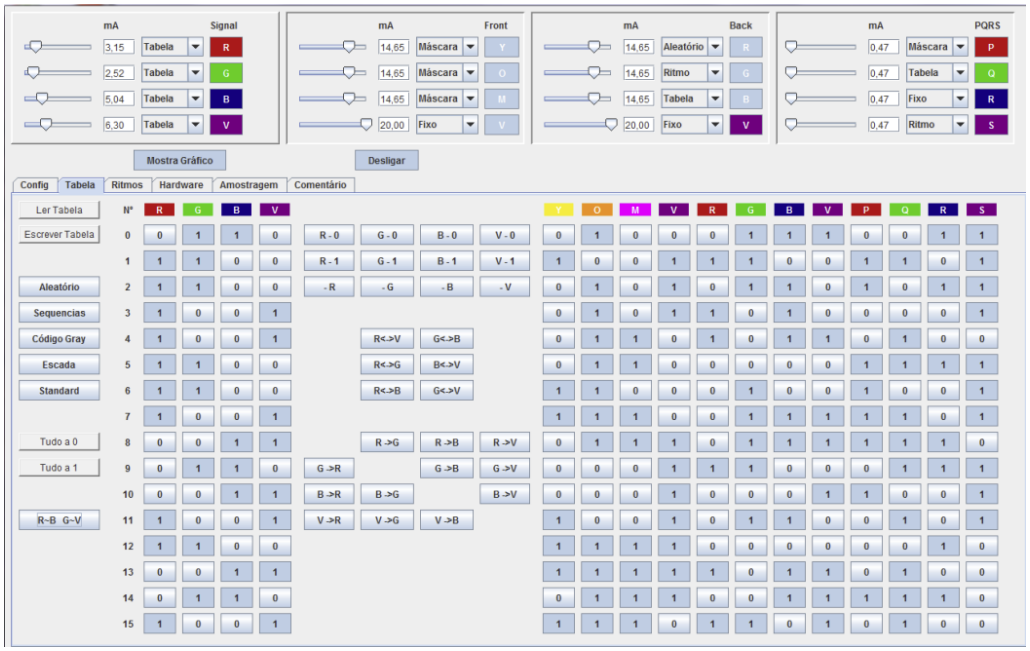

Figure 5.2: PiscaLed's interface.

It is possible to select in the program which channels are ON, and what will be transmitted by each. This is for example, if the vehicle is only present in a footprint with three overlapping channels. It is therefore necessary to build the frame structure discussed before in relation to the scenario position.

5.3 Header and Calibration Curve

Each step of the experimental results includes a header and calibration curve. The header is the same process explained in Chapter 3, being the same synchronization header [10101] at the start of each frame. The calibration curve supports the encoding and decoding techniques.

Using a binary sequence encoded between 0 and 15, the calibration curve is obtained. Obtaining the most optimal curve requires adjusting the intensity of each LED. Violet LEDs/channels have the least significant bit, with red LEDs/channels having the most significant bit.

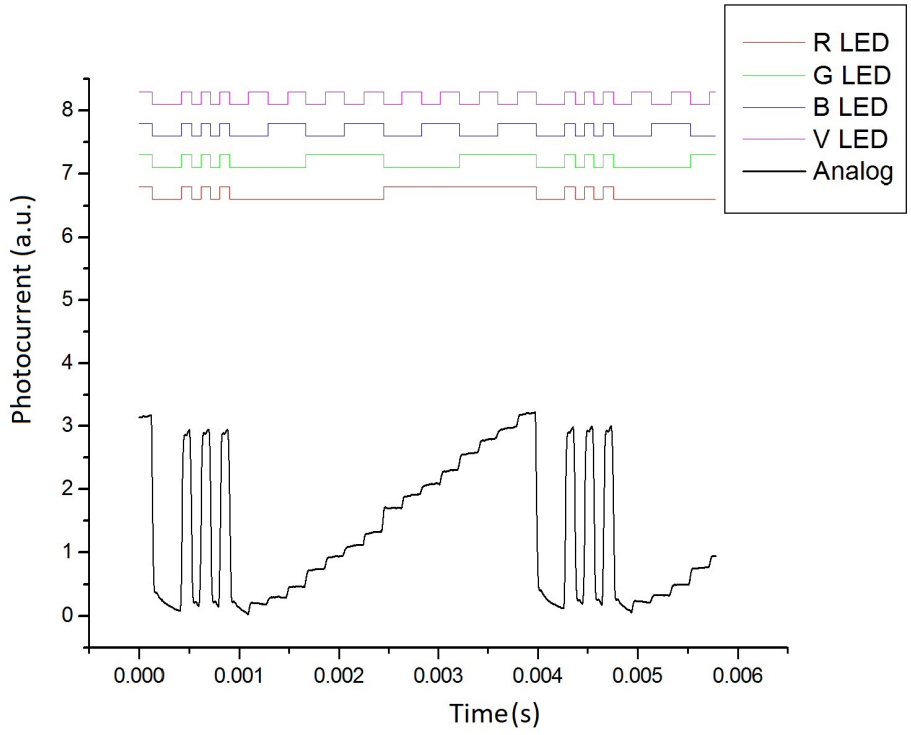

Figure 5.3: Calibration curve.

5.4 Tested Scenario

It is necessary to have a test scenario in order to perform a test. This experiment recreated the intersection discussed in Chapter 3 and used in simulation in Chapter 4.

Each of the seven cells has its own four LEDs, each with its own identification. The purpose of this experiment is to demonstrate how communication is handled when maneuvering at an intersection. Traffic messages sent in the experimental results are random, since in this experiment, the content of the message is not important, but how it is sent.

Results include the frame structure of a request message with the proper synchronization and calibration curve, as displayed in Figure 5.3.

A diagram of the proposed scenario can be found in Figure 5.4.

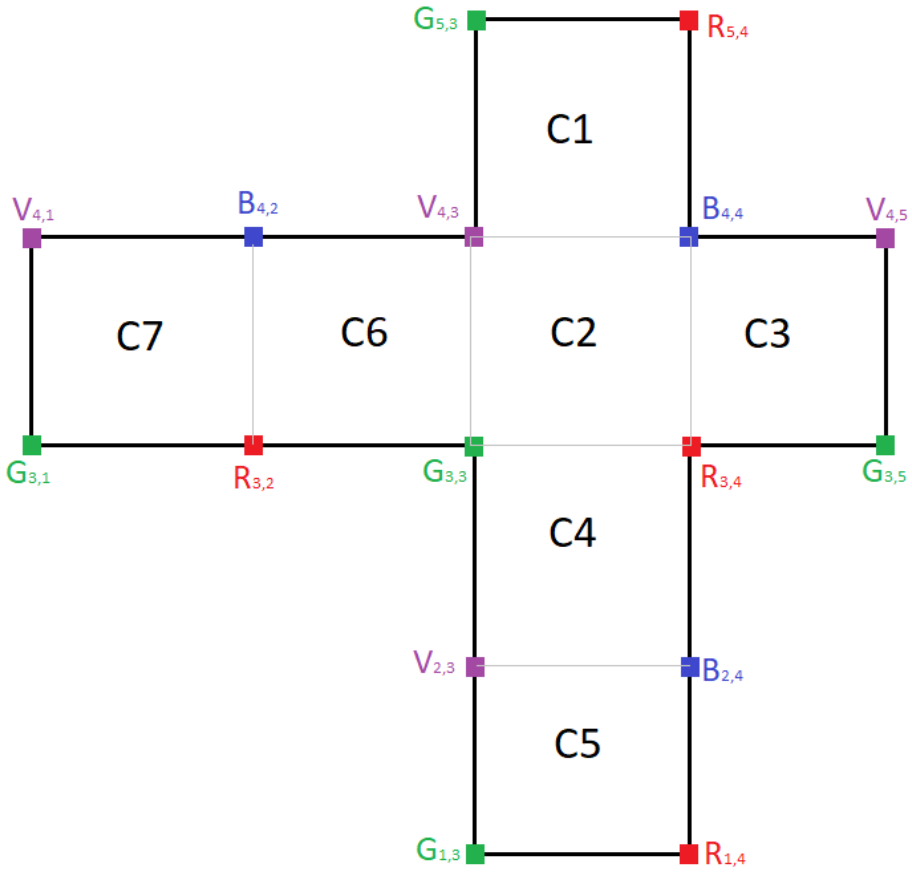

Figure 5.4: Tested scenario.

5.5 Experimental Results

Figure 5.5 illustrates the test scenario, which begins in cell C3. When the vehicle enters the intersection, cell C2, it begins its maneuver, occupying three different spots in the footprint before crossing the intersection and ending up in cell C4.

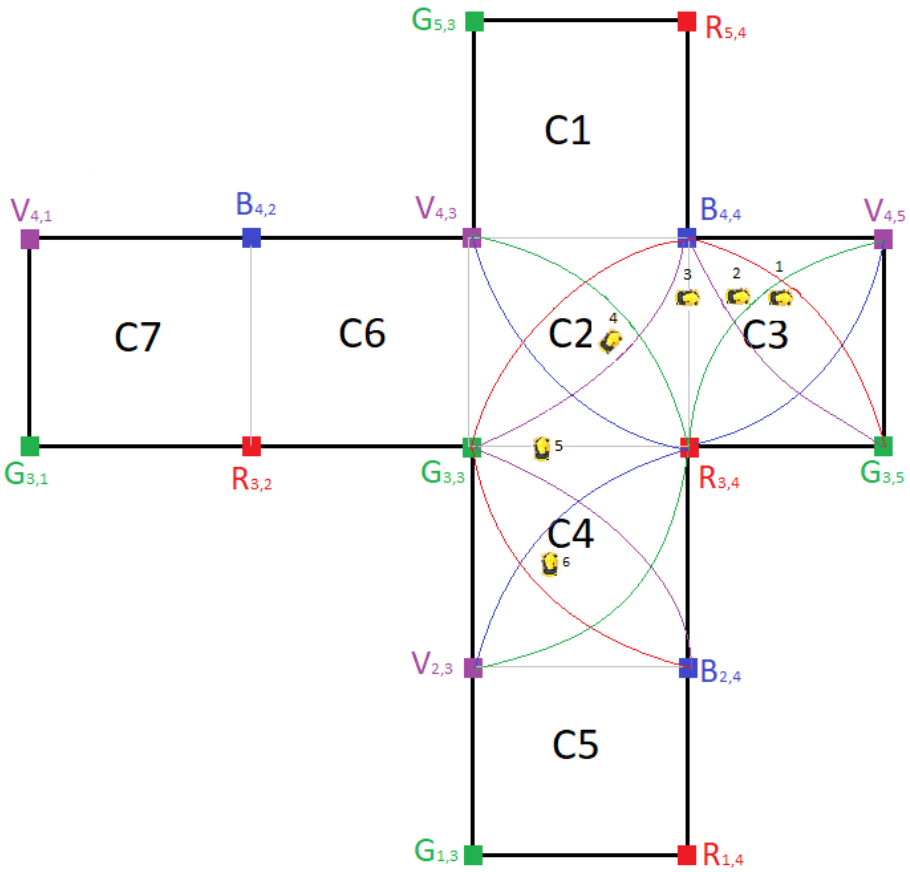

Figure 5.5: Proposed scenario, vehicle moving from East to South.

In cell C3, the results of the test at the first position are shown in Figure 5.6.

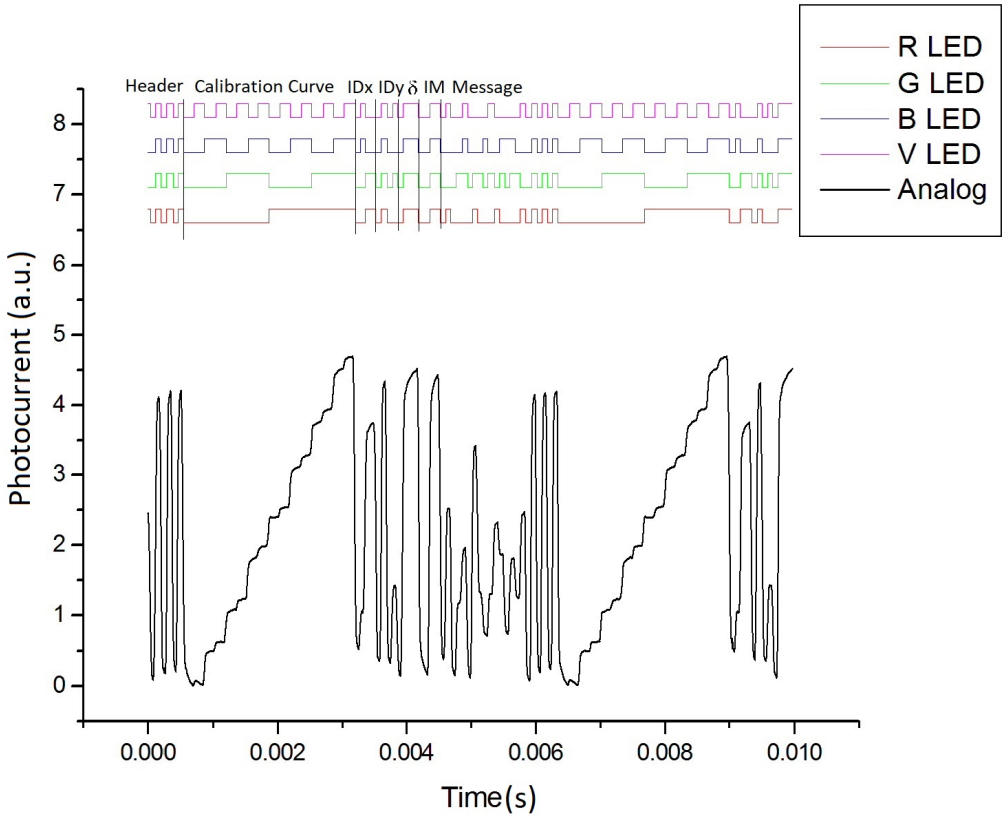

Figure 5.6: Results of the proposed scenario East to South (position 1), footprint #1.

It is assumed that the vehicle starts in the footprint #1 of the C3 cell, therefore it receives inputs from all channels. As discussed previously, the structure starts with the synchronization pattern, followed by the calibration curve. Following this, is the ID of the cell, which identifies each LED. $R_{3,4}$, $G_{3,5}$, $B_{4,4}$ and $V_{4,5}$ are the IDs. Since the vehicle is traveling west, the angle corresponds to [0111] in binary. The IM pattern is [11], since the vehicle is entering the intersection, so the message was sent from the IM to the vehicle. There is then a traffic message, which in this case is random, as said before.

Still in the same cell going straight, in the second position, the following results were obtained shown in Figure 5.7.

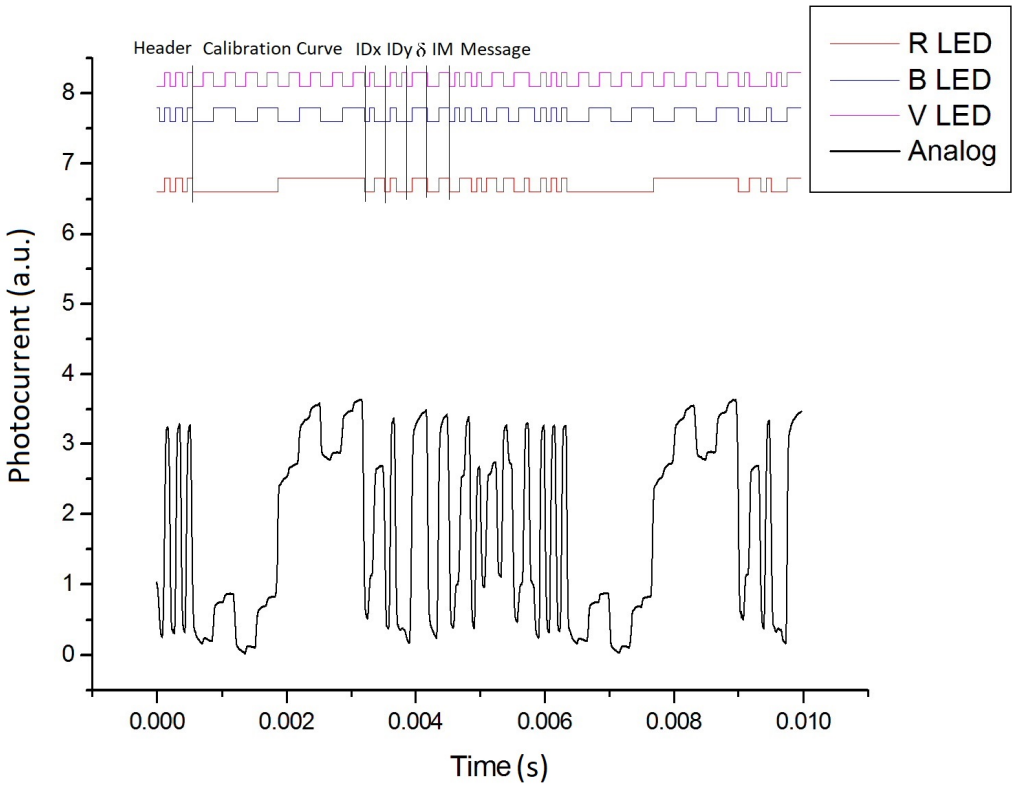

Figure 5.7: Results of the proposed scenario East to South (position 2), footprint #6.

The vehicle occupies the footprint #6 of cell C3, in this second position of the test scenario. There are only three channels in this position: red, blue, and violet. Since there are only three LEDs, the calibration curve does not have the 16 levels. Its IDs are $R_{3,4}$, $G_{UNKNOWN}$, $B_{4,4}$ and $V_{4,5}$, the angle is still 180°, which corresponds to 7, and the IM is [11], meaning that the message is sent by the IM to the vehicle.

Finally, the vehicle enter the C2 cell, where the maneuver begins, the position 3 results can be seen in Figure 5.8.

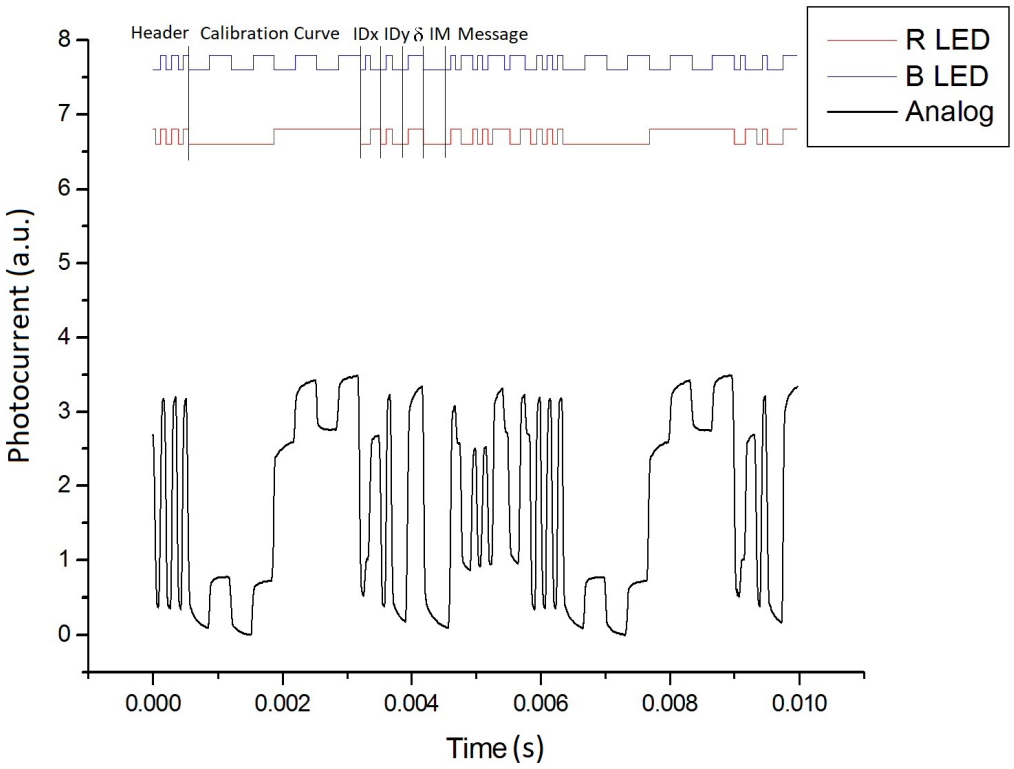

Figure 5.8: Results of the proposed scenario East to South (position 3), footprint #3.

Only Red and Blue are in range when the maneuver begins in footprint #3 in C2. The calibration curve differs when 4 channels are available, since only two channels are available. The channels IDs are: $R_{3,4}$, $G_{UNKNOWN}$, $B_{4,4}$ and $V_{UNKNOWN}$. Since the car has not started to turn, the angle remains 180º, which corresponds to 7. Since the vehicle entered the intersection, the IM is [00], meaning the message was sent by the vehicle to the IM.

Next, the vehicle is making a left turn, still on the same cell. The results are displayed in Figure 5.9.

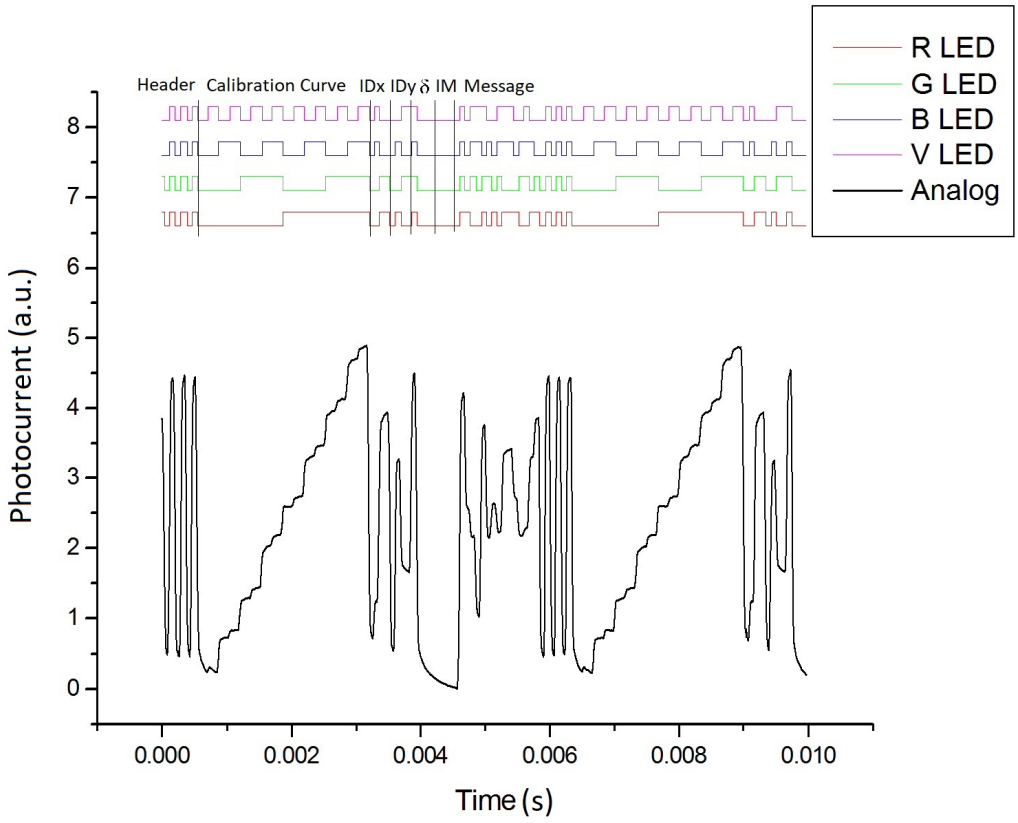

Figure 5.9: Results of the proposed scenario East to South (position 4), footprint #1.

Now being in the center of the intersection, meaning the cell C3 footprint #1, the vehicle is making a left turn. Since, it is the footprint #1, all of the four channels are in range. The channels IDs are: $R_{3,4}$, $G_{3,3}$, $B_{4,4}$ and $V_{4,3}$. Since the vehicle is making a left turn, the angle is 225° that corresponds to 8. The IM remains [00], meaning the message was sent by the vehicle to the IM.

The final position of the C2 cell is the position 5, when the maneuver ends in the intersection and starts to exit the intersection. The results of the position 5 are in Figure 5.10.

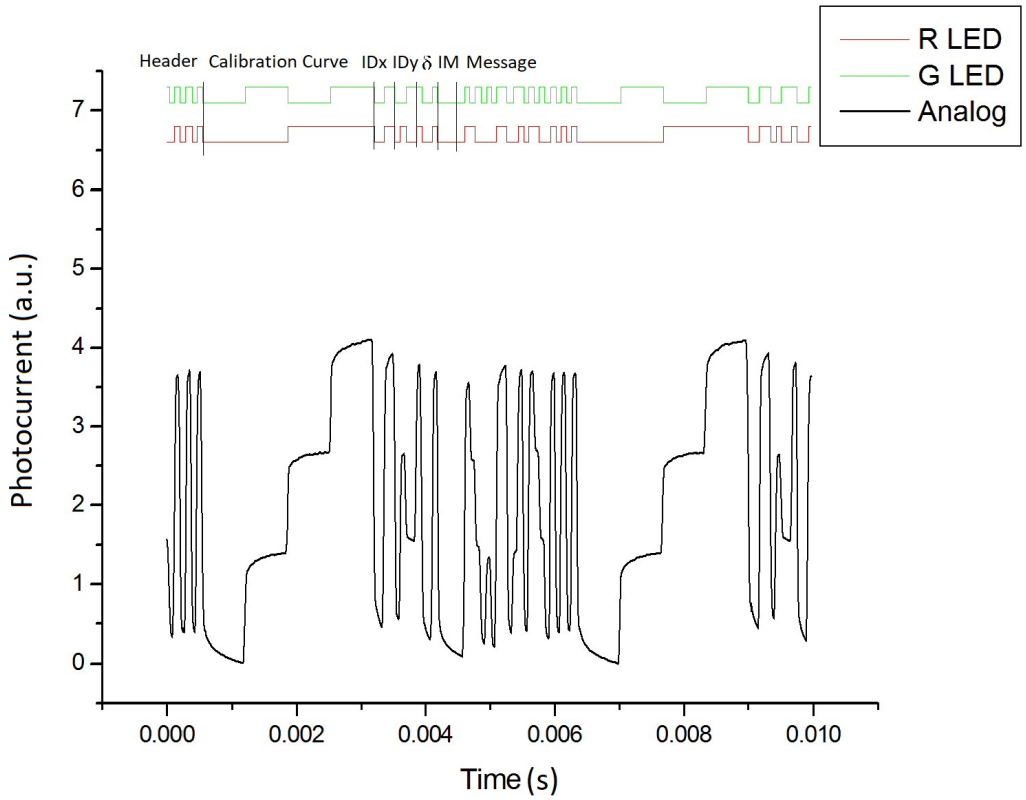

Figure 5.10: Results of the proposed scenario East to South (position 5), footprint #9.

Currently, in the last position of this cell, the vehicle is leaving the crossroad and is in footprint #9, where only the Red and Green channels are active. Its IDs are $R_{3,4}$, $G_{3,3}$, $B_{UNKNOWN}$ and $V_{UNKNOWN}$. The vehicle is now moving south, so the angle is now 270°, or [1001] in binary. Since the IM is [00], the message is sent by the vehicle to the IM.

Lastly, the final position 6, is when the vehicle enters the C4 position. These results are show in Figure 5.11.

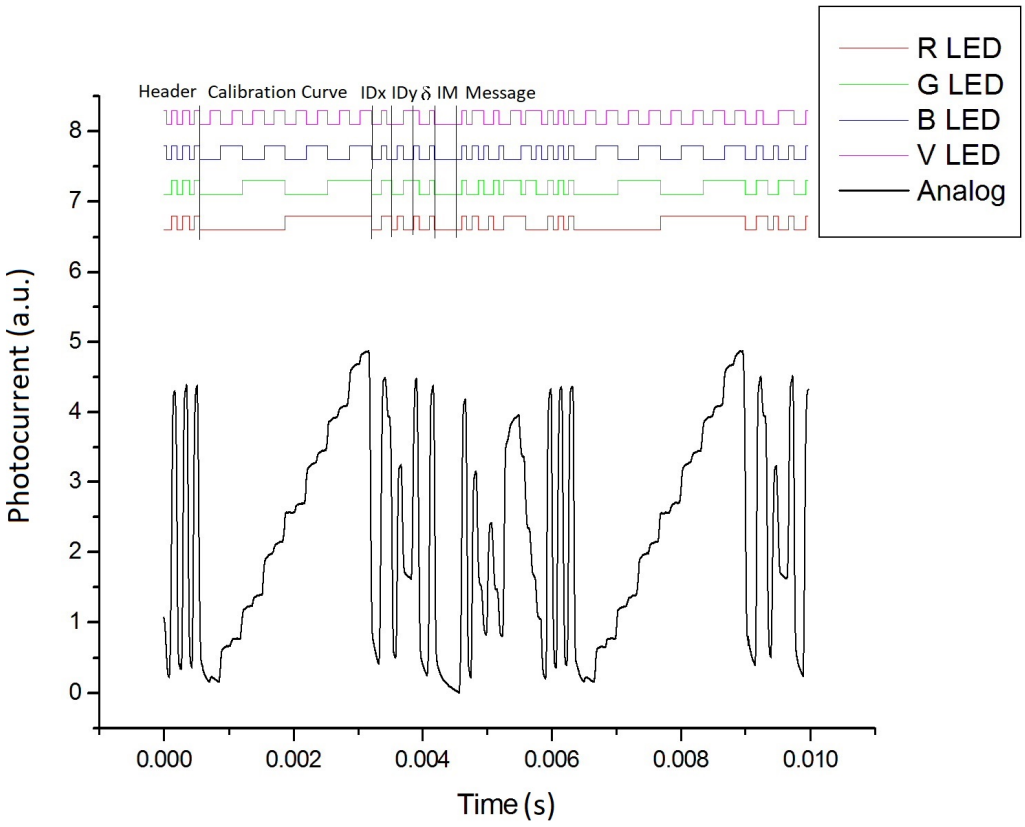

Figure 5.11: Results of the proposed scenario East to South (position 6), footprint #1.

Since the vehicle is in the center, footprint #1, all four channels are accessible. The IDs are: $R_{3,4}$, $G_{3,3}$, $B_{2,4}$ and $V_{2,3}$. Because the vehicle is leaving the intersection going south, the angle remains at 270°. As the IM is still [00], the message is sent by the vehicle to the IM.

These results enable us to understand how communication works and how it is conducted. Any maneuver performed by a vehicle follows the same process.

5.6 Decoding

Decoding is the final step in communication. Each LED/channel transmits a signal that is decoded from the multiplexed received signal. By doing so, it ensures that the vehicle and the infrastructure it communicates with are on the same page.

The received signal is from which the decoding process begins. The calibration curve is used by the vehicle (or infrastructure) to match each level of the incoming signal to the appropriate LED/channel combination.

As was previously established, the four LED/channels produce 16 different combinations, each of which corresponds to a certain calibration curve step. Each input step is compared to the calibration curve, and when a match is made, the appropriate LED/channel combination is shown.

An example is made with the results gathered in order to demonstrate how the decoding is carried out. A received bit with an amplitude of about 1 V is highlighted in Figure 5.12.

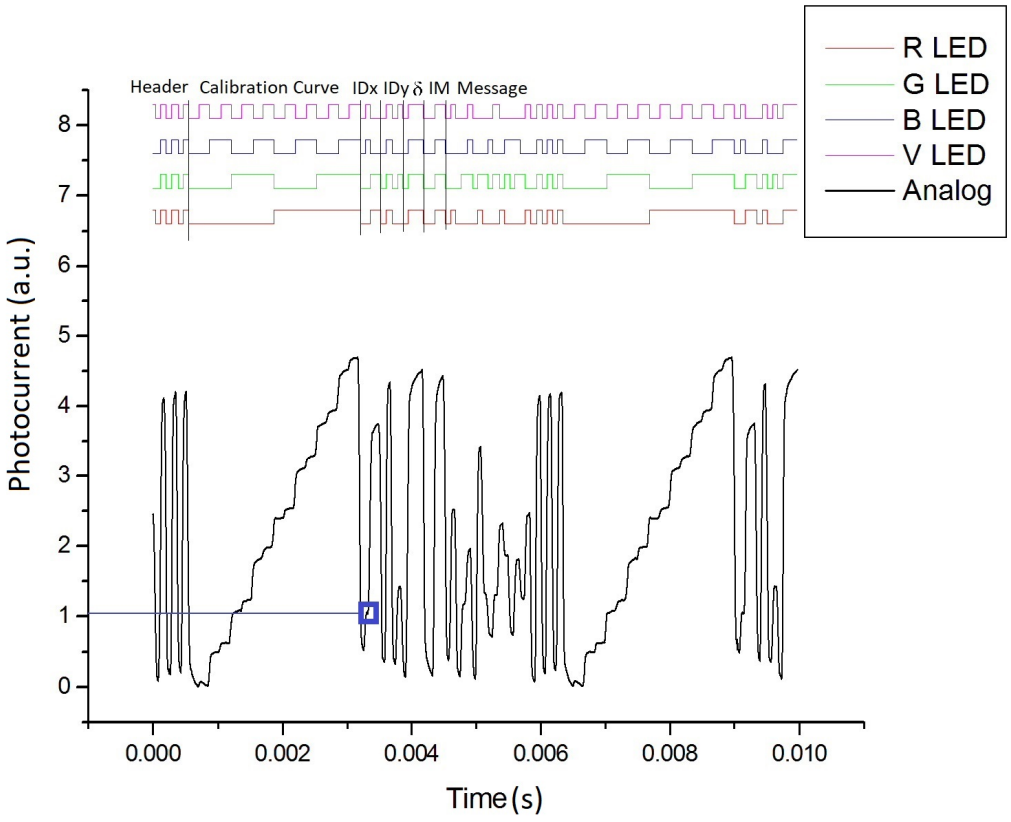

Figure 5.12: Figure 5.6 with a highlighted bit.

The ladder produced by the calibration should be compared to the bit's amplitude in Figure 5.12. The Figure 5.13 illustrates this.

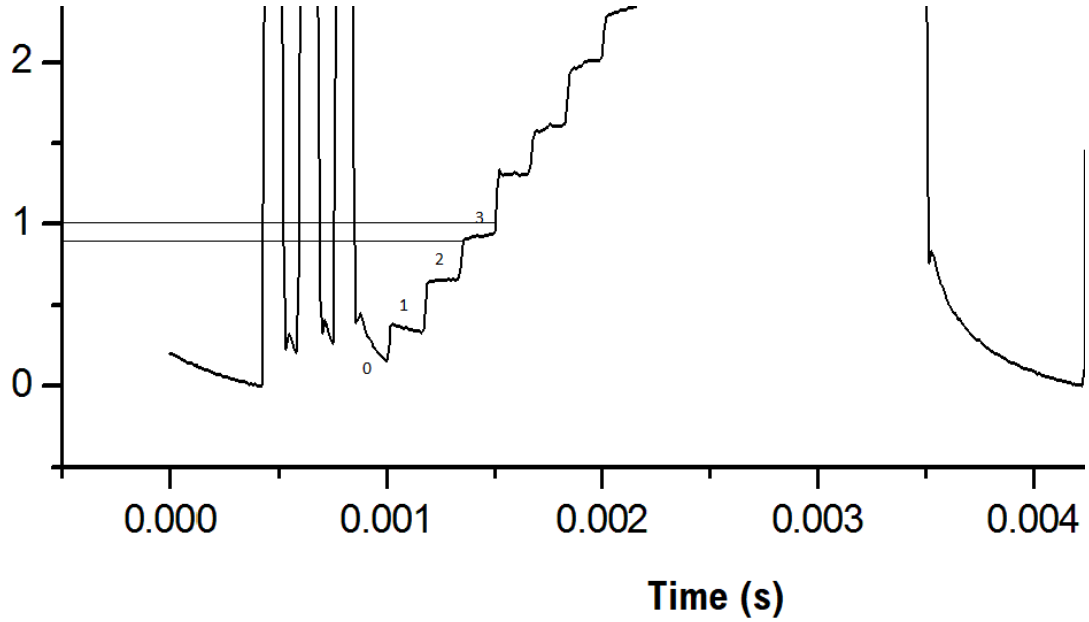

Figure 5.13: Calibration ladder in detail.

The third level, which corresponds to a combination of [0011] in binary, is the closest level to the recorded amplitude when analyzing the calibration levels of Figure 5.13. This value, according to the RGBV calibration, indicates that the Red and Green channels are off while the Blue and Violet channels are on.

Although it is the simplest decoding method, this technique can be extended to all bits.

6

Conclusion

This state of the art study concludes that OWC systems, primarily VLC systems, have evolved tremendously over the past decade. Systems like these are growing rapidly and being implemented in a wide variety of different areas, where they serve different purposes.

A specific area was studied in depth, which was VLC in autonomous technology, since this is the main technology involved in this work. Over the last few years, this technology has been implemented to reduce accidents, as well as increase the safety of drivers and pedestrians. In order to achieve this, V2V, V2I, and V2P communication are used.

These technologies have many problems and challenges, but there are some solutions that increase the cost or complexity of the system. Even with its problems, this technology still has numerous advantages over other technologies, such as RF technologies.

There is a wide variety of equipment and devices that are utilized in VLC systems. This includes a light source, which can either be a laser or an LED, typically, and each LED has a specific purpose for its wavelength. Receivers can be equipped with either a traditional photodetector or an imaging sensor, and both are used in different applications.

It is the purpose of the proposed work scenario to provide better security at traffic intersections, for which the vehicles and infrastructure are equipped with the

necessary equipment, mainly receivers and transmitters, in order to establish I2V, V2I, and V2V communication.

The transmission of data will be accomplished by white source tetrachromatic LEDs with one modulated channel, and the other three channels will be used for illumination. They are located at intersections in a grid formation, to avoid grid points overlapping. Footprints are formed by the overlap of transmission ranges of four channels. Each of the four channels creates nine different positions, numbered 1-9. Four channels overlap in footprint 1, three channels overlap in footprints 2, 4, 6, and 8, and two channels overlap in footprints 3, 5, 7 and 9.

In order to accomplish the proposed work, a software named OpticStudio Zemax was used. Using the same grid location for each LED, the intersection was built similarly to the proposed work in Chapter 3.

Using the software OpticStudio, it was possible to view the difference in intensity of each footprint, since the footprint 1, the center, is the overlap of the four channels, it is the more intense. Since each of the four channels have different power, the rest of the footprints are different in total power. The final scenario in the software shows a similar footprint map to the proposed work.

Due to the software limitations at this time, it was not possible to modulate the LEDs in order to transmit information. So to show how to communication works, it was done experimental results in lab.

It was proposed a scenario where the vehicle moves from East to South, where during this maneuver, it passes through several different cells, and different positions of said cells. It all of the vehicle movement, it was traced 6 different position throughout the scenario, to show the how the frame structure is built.

The start frame structure is composed by the synchronization header, which is [10101], followed by the calibration curve, which it can be different in some positions, due to the number of channels in reach. After the Identification of (x,y) of each channel is sent, followed by the angle δ of the car, which indicates where the car is moving to, after this the IM, that indicated if it is a V2I or I2V communication and finally the traffic message completes the frame.

Future developments can be made to this work. One of them can be in the software itself, if future versions of the software allow to modulate the channels, the experimental results could be improved and further explored in several new scenarios.

Bibliography

[1] Agon Memedi and Falko Dressler. Vehicular visible light communications: A survey. IEEE Communications Surveys Tutorials, 23(1):161–181, 2021.

[2] Manoj V. Bhalerao and S. S. Sonavane. Visible light communication: A smart way towards wireless communication. In 2014 International Conference on Advances in Computing, Communications and Informatics (ICACCI), pages 1370–1375, 2014.

[3] Mohsen Kavehrad. Sustainable energy-efficient wireless applications using light. IEEE Communications Magazine, 48(12):66–73, 2010.

[4] Zhaocheng Wang, Qi Wang, Wei Huang, and Zhengyuan Xu. Introduction to Visible Light Communications, pages 1–16. 2018.

[5] G. Pang, T. Kwan, Chi-Ho Chan, and Hugh Liu. Led traffic light as a communications device. In Proceedings 199 IEEE/IEEJ/JSAI International Conference on Intelligent Transportation Systems (Cat. No.99TH8383), pages 788–793, 1999.

[6] Hoa Le Minh, D. Obrien, G. Faulkner, Lubin Zeng, Kyungwoo Lee, Daekwang Jung, Yunje Oh, and Eun Tae Won. 100-mb/s nrz visible light communications using a postequalized white led. IEEE Photonics Technology Letters, 21(15):1063–1065, 2009.

[7] Johan Söderberg. Free space optics in the czech wireless community: Shedding some light on the role of normativity for user-initiated innovations. Science, Technology, & Human Values, 36(4):423–450, 2011.

[8] Jean-Philippe Javaudin and Martial Bellec. Omega project: On convergent digital home networks. In 2011 Third International Workshop on Cross Layer Design, pages 1–5, 2011.

[9] Birendra Ghimire and Harald Haas. Self-organising interference coordination in optical wireless networks. EURASIP Journal on Wireless Communications and Networking, 2012, 12 2012.

[10] Ryosuke Murai, Tatsuo Sakai, Hajime Kawano, Yoshihiko Matsukawa, Yukihiko Kitano, Yukio Honda, and Kenneth C. Campbell. A novel visible light communication system for enhanced control of autonomous delivery robots in a hospital. In 2012 IEEE/SICE International Symposium on System Integration (SII), pages 510–516, 2012.

[11] Yousef Almadani, David Plets, Sander Bastiaens, Wout Joseph, Muhammad Ijaz, Zabih Ghassemlooy, and Sujan Rajbhandari. Visible light communications for industrial applications—challenges and potentials. Electronics, 9:2157, 12 2020.

[12] Sachin Motwani. Tactical drone for point-to-point data delivery using laser-visible light communication (l-vlc). In 2020 3rd International Conference on Advanced Communication Technologies and Networking (CommNet), pages 1–8, 2020.

[13] Arnez Ardi, Ilham Aulia, Rizki Priramadhi, and Denny Darlis. Vlc-based car-to-car communication. Jurnal Elektronika dan Telekomunikasi, 20:16, 08 2020.

[14] Alin-Mihai Căilean, Mihai Dimian, and Valentin Popa. Noise-adaptive visible light communications receiver for automotive applications: A step toward self-awareness. Sensors, 20(13), 2020.

[15] Manuel A. Vieira, Manuela Vieira, Paula Louro, and Pedro Vieira. Cooperative vehicular systems: crossroad management through visible light. Optical Engineering, 60(11), 2021.

[16] Debbie Kedar and Shlomi Arnon. Non-line-of-sight optical wireless sensor network operating in multiscattering channel. Appl. Opt., 45(33):8454–8461, Nov 2006.

[17] A. Street, Paul Stavrinou, D. O'brien, and D. Edwards. Indoor optical wireless systems - a review. Optical and Quantum Electronics, 29:349–378, 03 1997.

[18] Dominic O'Brien, Hoa Le Minh, Lubin Zeng, Grahame Faulkner, Kyungwoo Lee, Daekwang Jung, YunJe Oh, and Eun Tae Won. Indoor visible light communications: challenges and prospects. In Arun K. Majumdar and Christopher C. Davis, editors, Free-Space Laser Communications VIII, volume 7091, pages 60 – 68. International Society for Optics and Photonics, SPIE, 2008.

[19] Tarik Borogovac, Michael B. Rahaim, Malika Tuganbayeva, and Thomas D. C. Little. "lights-off" visible light communications. In 2011 IEEE GLOBECOM Workshops (GC Wkshps), pages 797–801, 2011.

[20] Parth H. Pathak, Xiaotao Feng, Pengfei Hu, and Prasant Mohapatra. Visible light communication, networking, and sensing: A survey, potential and challenges. IEEE Communications Surveys Tutorials, 17(4):2047–2077, 2015.

[21] Rongqing Hui. Introduction to Fiber-Optic Communications. 2019.

[22] Yuki Goto, Isamu Takai, Takaya Yamazato, Hiraku Okada, Toshiaki Fujii, Shoji Kawahito, Shintaro Arai, Tomohiro Yendo, and Koji Kamakura. A new automotive vlc system using optical communication image sensor. IEEE Photonics Journal, 8(3):1–17, 2016.

[23] Jeffery C. C. Lo, S. W. Ricky Lee, Xungao Guo, and Huishan Zhao. Numerical prediction and experimental validation of multiple phosphor white led spectrum. In 2016 International Conference on Electronics Packaging (ICEP), pages 57–61, 2016.

[24] Lin liu. Led solar spectrum computer simulation based on non-dominated sorting genetic algorithm. Journal of Physics: Conference Series, 1578:012103, 07 2020.

[25] Seunghyun Lee, Philippe Gentet, Jungho Kim, Sungjae Ha, and Soonchul Kwon. Verification of the accommodative responses in viewing an on-axis analog reflection hologram. Open Physics, 19(1):119–126, 2021.

[26] Chu-Young Cho, Il-Kyu Park, Min-Ki Kwon, Ja Kim, Seong-Ju Park, Dong-Ryul Jung, and Kwang Woo Kwon. Ingan/gan multiple quantum wells grown on microfacets for white-light generation. Applied Physics Letters, 93:241109 – 241109, 01 2009.

[27] Erwin Setiawan, Trio Adiono, Isaac N. O. Osahon, and Wasiu O. Popoola. Experimental demonstration of visible light communication using white led, blue filter and soc based test-bed. In 2019 International Symposium on Electronics and Smart Devices (ISESD), pages 1–4, 2019.

[28] Haiqi Zhang, Aiying Yang, Lihui Feng, and Peng Guo. Gb/s real-time visible light communication system based on white leds using t-bridge cascaded pre-equalization circuit. IEEE Photonics Journal, 10(2):1–7, 2018.

[29] Chaofan Wang, Guoqiang Li, Yinaer Ha, Siqi Han, and Nan Chi. A 2.5gb/s real-time visible-light communication system b ased on phosphorescent white led. In 2019 7th International Conference on Information, Communication and Networks (ICICN), pages 140–145, 2019.

[30] Sezer Can Tokgoz, Noha Anous, Serhan Yarkan, Diaa Khalil, and Khalid A. Qaraqe. Performance improvement of white led-based vlc systems using blue and flattening filters. In 2019 International Conference on Advanced Communication Technologies and Networking (CommNet), pages 1–6, 2019.

[31] Thai-Chien Bui and Suwit Kiravittaya. Demonstration of using camera communication based infrared led for uplink in indoor visible light communication. In 2016 IEEE Sixth International Conference on Communications and Electronics (ICCE), pages 71–76, 2016.

[32] Jonathan J.D. McKendry, Dobroslav Tsonev, Ricardo Ferreira, Stefan Videv, Alexander D. Griffiths, Scott Watson, Erdan Gu, Anthony E. Kelly, Harald Haas, and Martin D. Dawson. Gb/s single-led ofdm-based vlc using violet and uv gallium nitride µleds. In 2015 IEEE Summer Topicals Meeting Series (SUM), pages 175–176, 2015.

[33] Neha Chitkara, Nidhi Chandoke, and Sujay Deb. Comparative study of different switch implementations for ook modulator. In 2014 International Conference on Devices, Circuits and Communications (ICDCCom), pages 1–4, 2014.

[34] Harald Haas, Jaafar Elmirghani, and Ian White. Optical wireless communication. Philosophical transactions. Series A, Mathematical, physical, and engineering sciences, 378:20200051, 04 2020.

[35] Khaled Shaaban, Md Hosne Mobarok Shamim, and Khadija Abdur-Rouf. Visible light communication for intelligent transportation systems: A review

of the latest technologies. Journal of Traffic and Transportation Engineering (English Edition), 8(4):483–492, 2021.

[36] Manuel Augusto Vieira, Manuela Vieira, Paula Louro, and Pedro Vieira. Redesign of the trajectory within a complex intersection for visible light communication ready connected cars. Optical Engineering, 59(9):1 – 16, 2020.

[37] Manuela Vieira, Manuel Vieira, and Paula Louro. Mux/demux sic receiver for visible light communications. Microsystem Technologies, 28, 07 2022.

[38] OpticStudio - Zemax.
https://www.zemax.com/pages/opticstudio.
Accessed: September 2022.

[39] Murat Uysal, Farshad Miramirkhani, Omer Narmanlioglu, Tuncer Baykas, and Erdal Panayirci. Ieee 802.15.7r1 reference channel models for visible light communications. IEEE Communications Magazine, 55(1):212–217, 2017.

[40] Farshad Miramirkhani and Murat Uysal. Channel modeling and characterization for visible light communications. IEEE Photonics Journal, 7(6):1–16, 2015.